TECHNOLOGICAL CHANGE AND CULTURAL RESISTANCE AMONG SOUTHEAST IBERIAN POTTERS: ANALYTICAL CHARACTERISATION OF EARLY IRON AGE POTTERY FROM CASTELLAR DE LIBRILLA

Benjamín Cutillas-Victoria, Jaume Buxeda i Garrigós, Peter M. Day

Archaeological and Anthropological Sciences (2021) 13:174

Technological change and cultural resistance among southeast Iberian potters: analytical characterisation of Early Iron Age pottery from Castellar de Librilla.

Benjamín Cutillas-Victoria. Grupo de Investigación en Arqueología (E041-02), Facultad de Letras, Universidad de Murcia, Spain (benjamin.cutillas@um.es)
Jaume Buxeda i Garrigós. Cultura Material i Arqueometria UB (ARQUB, GRACPE), Dept. d'Història i Arqueologia, Facultat de Geografia i Història, Universitat de Barcelona, Catalonia, Spain (jbuxeda@ub.edu)
Peter M. Day. Institute of Nanoscience and Nanotechnology, National Centre for Scientific Research 'Demokritos', Greece / Department of Archaeology, University of Sheffield, U.K. (p.m.day@sheffield.ac.uk)

Abstract

The beginning of relationships between autochthonous communities and Phoenicians from the earliest contacts in the 8th century BC made possible the exchange of ideas, technologies and people. This work analyses the development of the Early Iron Age potteries of the Iberian Southeast, the impact of the Phoenician presence and the agency that these local groups exercised on their ceramic assemblages until the 5th century BC. The incorporation of new archaeometric data from Castellar de Librilla, one of the region's main autochthonous settlements, has been essential to improve our approach to these cultural encounters. A total of 63 representative individuals have been analysed through X-ray fluorescence (XRF), X-ray diffraction (XRD), thin-section petrography and scanning electron microscopy (SEM). The results point to the local production of ceramics previously considered as Western Phoenician pottery, and to the degree of specialisation of the potters established in the autochthonous settlements, combining traditional and new techniques from early in the period of contact.

Keywords: Iberian Southeast, Early Iron Age pottery, chemical analysis, mineralogical analysis, technology, cultural encounter, agency.

1. Introduction

The first Phoenician presence in the Iberian Peninsula dates to at least the 9th century cal BC (Nijboer and van der Plicht 2006; Fernández and Rodríguez 2007; Sánchez et al. 2011). The appearance of wheel-made ceramics among Late Bronze Age vessels is one of the main indicators of the beginning of occasional contacts that led subsequently to the establishment of permanent colonies. The consumption of Phoenician containers and other ceramic vessels by inland communities then testifies to the consolidation of economic relations between autochthonous settlements and the coastal colonies. Over time these new forms become a familiar component integrated with local-style pottery. However, this process went beyond the materiality of the products, given that the potters of the autochthonous settlements adopted wheel throwing as a forming

method and started to employ double chamber kilns. Clearly the technology of both forming and firing underwent substantial change, with the colonial presence acting as a catalyst.

Despite these substantial technological innovations, some handmade vessels seem to have remained unchanged until the end of the 6th century BC, following a manufacturing tradition that can be traced back to the Late Bronze Age in the region. As a result of this cultural encounter, mixed ceramic repertoires in which handmade and wheel-made pottery vessels shared domestic spaces and workshops were common; a situation that was not exclusive to the autochthonous settlements but is also noticed in the colonial communities with the introduction of handmade ceramics from their earliest phases.

At some sites, the prolonged coexistence of these two production traditions has served to promote a picture characterised by a hypothesised duality of wheel-made ceramics seen as imports from Phoenician workshops, in contrast to handmade products, considered the result of autochthonous Early Iron Age pottery traditions. This dichotomy tends to be extended to the control of the new forming methods and kiln firing, thought to be the domain of colonial potters and only belatedly transmitted to autochthonous artisans; a situation that clearly shows how the colonial situations tend to be reduced to a relatively simple binary opposition between colonisers and colonised (van Dommelen 1998). The expression of these *technological boundaries* is evident in cases such as the identification of certain production areas located in autochthonous settlements that have been described as 'Phoenician districts' (González Prats 1983, 2011), ignoring other possible processes, such as hybridisation or the agency of local potters.

For the Iberian Southeast, this encounter began in the 8th century BC with the establishment of the Phoenician colonies of the mouth of the Segura river (Rouillard et al. 2007; González Prats 2011; García Menárguez and Prados 2014) and the occupation of different coastal promontories and islands in the Bay of Mazarrón (Ros 2017). From that moment, wheel-made pottery strongly increases its presence in ceramic assemblages of autochthonous settlements, comprising more than 50% of the assemblage in some instances, as in Castellar de Librilla at the end of the century (Ros 1989). However, the double chamber kilns identified thus far date somewhat later, to the 6th century BC (Ros 1989; Martínez 2006). This chronological discrepancy has favoured the wheel's association with ceramics produced by potters in the Phoenician colonies, using newly introduced forming methods, and excluded the agency of autochthonous potters, especially at this early time of the 8th and 7th centuries BC.

It is with this background that we present the analysis of the ceramic repertoires identified in the potter's workshop of Castellar de Librilla (Librilla, R. Murcia, Spain), one of the main settlements of this period in the region (Fig. 1). Applying a methodological approach focused on archaeometric techniques at this well-known site (Ros 1989; Cutillas and Ros 2020), the first objective was the chemical and mineralogical characterisation of the pottery assemblage. The sample includes handmade and wheel-made ceramics from the phases pre-dating the potter's kiln excavated at Castellar de Librilla, in order to examine the development of local pottery production and consumption at the site from the Late Bronze Age to the Early Iron Age. The results have been cross-referenced with archaeological data to define the chemical reference groups (Buxeda i Garrigós and Madrid 2017) and petrographic fabrics (Whitbread 1989, 1995; Quinn 2013) associated with this production environment, highlighting the local manufacture of products considered *a priori* as Western Phoenician but made in the settlement or its surroundings from its earliest phases.

1.1 Archaeological context of the site

Castellar de Librilla lies in the extensive inland basin of the Guadalentín-Segura rivers, the main natural corridor that runs across much of the southeast of the Iberian Peninsula, and at its junction with the Rambla de Las Moreras, which connects it to the Bay of Mazarrón. Its foundation dates back to the 9th century BC (Cutillas and Ros 2020), prior to the Phoenician colonisation and at the time of substantial territorial reorganisation that took place during the Late Bronze Age, as a result of the intensification of contacts and exchange with Atlantic, Central Mediterranean and peninsular networks. As in other contemporary settlements, such as Peña Negra in Crevillente (González Prats 1983; Lorrio et al. 2016), the foundation of these main settlements and the intensification of local production and economic activity fed into the increased prominence of the region during the 10th and 9th centuries BC and helps to explain the later Phoenician interest in settling the coastal areas.

Castellar de Librilla's internal layout followed a polynuclear model from its foundation, with several sectors occupied on both sides of the Rambla de Algeciras (Fig. 2). The settlement's best-known sector, excavated from 1980 to 1986, is located on the east side of the stream, where several urban areas and workshops were identified. Their chronology spans from the 9th to the 4th century BC (Ros 1989). A surface survey carried out in 2019 testified to a settlement of even greater extent than previously suspected, with new areas of occupation identified on the middle and upper slopes of the mountain range and important fortified structures and terrace walls (Cutillas and Ros 2020). On the west side, the urban occupation is concentrated in Cabezo de la Fuente del Murtal, partially excavated in the nineties (García Blánquez 1996; Lomba and Cano 2002), revealing a sequence of occupation synchronous to that identified in Castellar. This sector truly stands out for the fortified structures located on its summit, a massive fortress with bastions dating from the 6th century BC and the Iberian tower in the summit's northeast sector, under excavation since 2018.

In the period of its maximum extent, contemporary with the most prosperous phase of Phoenician trade networks between the 7th and 6th centuries BC, this settlement occupied more than 45 ha (Cutillas and Ros 2020). Although the model of urban development was polynuclear, the different districts or sectors formed part of the same socio-political entity. This arrangement also explains the possible centralisation of transformative activities in the settlement, concentrated in the area identified as Sector I (Ros 1989) where a metallurgical furnace dedicated to iron work was built in the initial phase. A second metallurgical furnace and a pottery kiln were then constructed at the end of the 7th or early 6th century BC. The concentration of these structures for craft production enables the identification of this sector as a district where artisan crafts were concentrated and reveal the availability of resources that exist in the surrounding areas of the settlement - water springs, clay and mining outcrops, wood charcoal - that underpin the development of those activities (Ros 1989).

The kilns' continuity during the second half of the 6th to the beginning of the 5th century BC reveals the importance of this area and activities for the settlement. During this period, in the Iberian Southeast, there was a weakening of trade systems, an abandonment of Phoenician colonies and the disappearance or contraction of the autochthonous settlements. However, this area of Castellar de Librilla and its metallurgical and pottery kilns continued in operation with their productive traditions, even in this time of

demographic decline and transition to a new urban model. Indeed, this resilience lasted until the 4th century BC within the new ambience in the Western Mediterranean during the Second Iron Age.

(Fig.1) & (Fig.2)

1.2 Local geology

Castellar de Librilla is located in the Neogene basin of Alhama de Murcia - Alcantarilla. This area is in the central sector of the southeast of the Iberian Peninsula and in the east Baetic System. It is also located on the Alhama de Murcia Fault, one of the longest faults in the Eastern Baetic Shear Zone (Herrero et al. 2017) that accommodates part of the NW-SE convergence between the Eurasian and Nubian plates in the Western Mediterranean (Argus et al. 2011). The geomorphological evolution of the environment is highly affected by aridity and erosive processes that began at least from the third millennium BC (Carrión et al. 2010; Navarro et al. 2014). Among these, the most important episodes for the area occurred during the Sub-Atlantic stage when a fast erosive crisis accentuated by torrential rains took place; the result was the Holocene glacis' incision of the lower Guadalentín and the Rambla de Algeciras to a depth of 20 m (Calmel-Ávila 2000).

The mountain range in which the site and its surroundings are located (Fig. 3) is almost entirely made up of clay-rich sedimentary marls with interleaved gypsums associated with the Upper Tortonian and the Terminal Miocene. However, some outcrops correspond to medium and low-grade regional metamorphism rocks –mainly phyllites and quartzites– that appear as a consequence of the fault movements (Ros 1989). In summary, the local geology is mainly sedimentary with regular appearances of metamorphic materials (Fig. 3), a type of composition and a range of aplastic inclusions not significantly different from those identified among the ceramics locally produced.

(Fig.3)

2. Sample choice and methods

The samples analysed from Castellar de Librilla (n = 63, Table 1) comprise representative ceramics from Sector I of the settlement. The individuals analysed are ascribed to the Lib-IV and Lib-V phases (end of the 7th or early 6th century to the beginning of the 5th century BC), when the kiln was active, and to phases Lib-II and Lib-III, from the end of the 8th to the 7th centuries BC. Moreover, seven individuals were recovered from stratigraphic units related to combustion chamber of the pottery kiln, and two from its dump (Table 1), representing different types of ceramics under study. The main change between the two periods was the remodelling of the LBA and EIA structures of this area of the settlement for the building of a new industrial area with two metallurgical furnaces and the potter's kiln M (Ros 1989). This transformation explains why the origin of the samples from the Lib-IV and Lib-V phases is closely related to the pottery kiln (Table 1)), while the rest of the samples are related to the LBA and EIA living spaces that existed prior to this structure.

The inclusion of ceramics from older phases before the kiln construction was designed to shed light on whether there was already ceramic manufacture in the site. At a technological level, such a diachronic study was essential to determine if there had been changes in pottery practice parallel to the urban and sociocultural modifications that the settlement itself testifies to (Ros 1989; Cutillas and Ros 2020). For this reason, a broad sample composed of both wheel-made and handmade ceramics has been studied to

characterise locally produced pottery during this period: as for the former, examples of grey pottery, red slipped vessels and amphora stand out; as for the latter, cooking pots are the main type analysed, along with triangular supports identified as kiln furniture.

(Table.1)

After thorough macroscopic study of each individual, a combined archaeometric approach was designed to include chemical, mineralogical and petrographic analysis to define the pastes and clays associated with local pottery production. The chemical composition of 57 samples was studied using X-ray fluorescence (XRF). The superficial layers were mechanically removed, and the samples milled in a tungsten carbide cell mill Spex Mixer mod. 8000. The chemical composition was determined from powder previously dried in an oven for 12 h at 105 °C. To determine the major and minor elements, two 30 mm glass bead replicates were made by mixing 0.3 g of dried sample with 5.7 g of lithium tetraborate ($Li_2B_4O_7$) flux (1/20 dilution) and 5 mg of lithium iodide (LiI) as a release agent. This mixture was homogenised and deposited in a 95%Pt-5%Au crucible and melted in a fully automatic bead preparation system PANalytical Perl'X-3 at a temperature of 1125 °C. To determine trace elements pressed powder pellets were made using 6 g of specimen mixed with 2 ml of a binding agent solution of n-butyl methacrylate synthetic resin (Elvacite® 2044) in acetone at 20 % by mass. This mixture was manually homogenised in an agate mortar to dryness and placed on a base of boric acid (H_3BO_3) in an aluminium vessel of 40 mm diameter that was subjected to a pressure of 200 kN for a period of 60 s using a Herzog press.

The quantification of the concentrations was performed using an Axios^{mAX}-Advanced PANalytical spectrometer with an Rh excitation source calibrated by a suite of 56 international Geological Standards. Interferences were taken into consideration, and matrix effects were corrected using the PANanalytical Pro-Trace software for trace elements. The elements determined were: Na_2O, MgO, Al_2O_3, SiO_2, P_2O_5, K_2O, CaO, TiO_2, V, Cr, MnO, Fe_2O_3 (as total Fe), Co, Ni, Cu, Zn, Ga, Rb, Sr, Y, Zr, Nb, Mo, Sn, Ba, Ce, W, Pb and Th. Major and minor elements are expressed as concentrations of oxides in percentage by mass (% m/m; also referred to as wt %). Trace elements are expressed as concentrations of elements in μg/g (or ppm —parts per million). Loss on ignition (LOI) (expressed as % m/m) was determined by firing 0.3 g of the dried specimen at 950 °C for 3 h. Calcinations were carried out in a Heraeus muffle model M-110, by using a heating rate of 3.4 °C/min and free cooling. Thus, the sum of major, minor, trace element concentrations and LOI, is located within a range of 98—102 %.

X-ray diffraction (XRD) was applied to characterise the mineralogical composition of all 57 individuals analysed by XRF. The previously prepared powder specimens were manually side-loaded and pressed with frosted glass in a cylindrical sample holder of 27 mm diameter and 2.5 mm in height. Measurements were made using a Bragg-Brentano geometry diffractometer PANalytical 'X'Pert PRO MPD Alpha-1 (radius = 240 mm) using the Ni-filtered Cu Kα radiation (λ = 1.5418 Å) at a working power of 45 kV and 40 mA, equipped with an X'Celerator detector (active length = 2.122°). Measurements were taken from (5 to 80)°2θ with a 0.026° step size and an acquisition time of 50 s, spinning the sample at 1 Hz. Evaluations of the crystalline phases present in each specimen were performed using the PANalytical X'Pert HighScore Plus software package that includes the database of the International Centre for Diffraction Data–Joint Committee of Powder Diffraction Standards, 2006 (ICDD–JCPDS).

The petrographic and mineralogical analysis of thin sections was carried out using a Zeiss Axiophot polarising microscope, working with a magnification between x20 and x200. To prepare the thin section, each sample was impregnated with epoxy resin, mounted using Norland Optical UV glue (Norland), and sectioned using a Buehler Petro thin system (Buehler). The thin sections were finished by hand, using a silicon carbide until reaching a thickness of 30 μm when the quartz presents a grey-white interference colour. Description of individuals and group formation follows the description system of the structure and components developed by Whitbread (1989, 1995; Quinn 2013). An Olympus SC-50 digital camera attached to the microscope was operated by specific software to take the photomicrographs. In total, 56 individuals were examined by optical microscopy, including the 6 samples without chemical characterisation.

Finally, analysis with scanning electron microscopy (SEM) has been applied to 15 individuals to represent the different chemical groups and fabrics. Samples were analysed with a JSM-6510LV Scanning Electron Microscope in high vacuum conditions attached to an energy-dispersive X-ray spectrometer (EDX), being analysed later through an acceleration voltage of 20 kV with a beam current of 1 nA and 100 s per microanalysis. Bulk specimens were fixed on metal specimen stubs using silicone adhesive, and the non-conductive ceramic specimens were made conductive. Colloidal silver paint was applied on excess silicone adhesive and lateral sides of the ceramic bulk specimen. The specimen surface was then coated with a thin carbon film (~ 10 nm) by vacuum evaporation.

3. Results

3.1 Chemical Analysis

The results of elemental concentrations of Castellar de Librilla samples analysed by XRF (Table 2) correspond with a special case of the projective d+1-dimensional space where the projective points are projected into the simplex $\mathbb{S}^d$. Points are represented by homogeneous coordinates that have a constant sum k ($k \in R_+$),

$$\mathscr{C}(\mathbf{w}) = \mathbf{x} = [x_1,..., x_d, x_{d+1}] \mid x_i \geq 0 \text{ (i = 1,..., } d, d+1), x_1 + \ldots + x_d + x_{d+1} = k,$$

(in this current case, k = 100). The projective points' vector space is the positive orthant. Both they and their projections in the simplex follow a multiplicative model with a metric of logarithmic intervals. Hence, for the statistical data treatment, the raw concentrations have been alr (additive log-ratio) transformed, according to

$$\mathbf{x} \in \mathbb{S}^d \rightarrow \mathbf{y} = \ln\left(\frac{\mathbf{x}_d}{x_{d+1}}\right) \in \mathbb{R}^d$$

being $\mathbb{S}^d$ the d-dimensional simplex and $\mathbf{x}_d = [x_1,...,x_d]$. They have also been clr (centred log-ratio) transformed following the equation

$$\mathbf{x} \in \mathbb{S}^d \rightarrow \mathbf{z} = \ln\left(\frac{\mathbf{x}}{g(\mathbf{x})}\right) \in \mathbb{H} \subset \mathbb{R}^{d+1}$$

being $\mathbb{S}^d$ the d-dimensional simplex, g($\mathbf{x}$) the geometric mean of all d+1 components of $\mathbf{x}$ and $\mathbb{H} \subset \mathbb{R}^{d+1}$ a hyperplane vector subspace of $\mathbb{R}^{d+1}$ (Aitchison 1986; Buxeda i Garrigós 1999; Egozcue and Pawlowsky-Glahn 2011; Martín-Fernández et al. 2015; Buxeda i Garrigós 2018). Furthermore, some of the major and

minor elements were discarded for statistical data treatment because of various problems: Co and W due to the possible contaminations from the tungsten carbide cell of the mill; Mo and Sn by low analytical precision and P_2O_5 given that several post-depositional processes easily alter it. Sr was also disregarded due to high and irregular concentrations appearing in several individuals possibly because of the post-depositional crystallisation of Celestine ($SrSO_4$), identified by SEM. The elements retained for statistical data treatment, performed with R (R Core Team 2021), are: Na_2O, MgO, Al_2O_3, SiO_2, K_2O, CaO, TiO_2, V, Cr, MnO, Fe_2O_3, Ni, Cu, Zn, Ga, Rb, Y, Zr, Nb, Ba, Ce, Pb and Th.

(Table.2)

The first analysis carried out was to calculate the variation matrix that completely determines the covariance structure of compositional data and provides the total variation (*vt*) of the analysed ceramic assemblage (Fig. 4) (Aitchison 1986; Buxeda i Garrigós and Kilikoglou 2003; Buxeda i Garrigós and Madrid 2017). The overall data set value is equal to 1.77, which means a high value that indicates the existence of a polygenic group. The compositional evenness plot reveals that the elements that introduce more variability are MnO, Pb, Na_2O, MgO, and CaO. Contrarywise, Th and Y are the elements that introduce less variability. The influence of CaO is essential to differentiate the calcareous and low-calcareous ceramics. Calcareous clays were used mainly for wheel-made products and low calcareous clays for handmade ceramics.

This dichotomy is reflected in the dendrogram, resulting from cluster analysis based on the square Euclidean distance and the centroid agglomerative algorithm (Fig. 5), where the difference between calcareous (5%-6% < CaO < 15%-25%) and low calcareous pottery (CaO < 5%-6%, in some cases below 2%) determine the two main branches. From this first division, the dendrogram shows four main clusters, CLI-A to CLI-D, which are also identified by principal component analysis (PCA) performed on the same sub-compositions using the singular value decomposition of the double centred clr transformed data (van de Boogaart and Tolosana-Delgado 2013) (Fig. 6).

CLI-A is the first and largest of the identified clusters, including 37 ceramic individuals (Table 3). Its total variation is relatively low (*vt* = 0.32), which suggests that this assemblage could have a monogenic character according to the principles established by Buxeda and Kilikoglou (2003) where the variability of similar compositions should be positioned around 0.3. The broad ceramic assemblage included - grey ceramic, red slip ware, amphorae, triangular supports, handmade pots - support this consideration given that the *vt* of the cluster continues to be relatively low. However, in the PCA two chemical groups have been differentiated: CLI-A1 and CLI-A2. The groups' chemical compositions are similar, but some differences that allow their separation have been distinguished, mainly in terms of Na_2O. Group CLI-A2 (n = 8; vt = 0.22) exhibits, in general, lower Na_2O concentrations than group CLI-A1 (n = 29; vt = 0.25). Individuals CLI033 and 56, recovered from the combustion chamber of the pottery kiln, are classed in CLI-A1, while individuals CLI023, 55, and 58, recovered from the same contexts, are classed in CLI-A2.

Group CLI-B (*vt* = 0.21) includes three wheel-made ceramics intended for tableware. Its chemical composition is not excessively different from that identified of the previous group, but their MgO values above 4.5% and up to 5.7% contrast (Table 3). Individual CLI024, recovered from the kiln dump, is classed in this group.

(Fig.4) & (Fig.5)

(Fig.6)

Clusters CLI-C1, CLI-C2 and CLI-D group the individuals of low or very low calcareous ceramics (Table 3). Cluster CLI-C comprises ten handmade individuals, with a total variation of 0.49. However, total variation in handmade coarse products sharing a common origin can easily rise to around 0.6/0.7, due to the quantity and size of aplastic inclusions (Buxeda i Garrigós et al. 2001; Albero and Cau 2016; Cau et al. 2019). Cluster analysis and PCA support two different chemical groups within this cluster: CLI-C1 (n = 3; *vt* = 0.25) and CLI-C2 (n = 7; *vt* = 0.34). Both groups show similar chemical compositions, but group CLI-C2 presents lower relative values for CaO than group CLI-C1. Individual CLI046, recovered from the kiln dump, is classed in group CLI-C2.

The three individuals of the CLI-D cluster seem to conform to a monogenic group whose total variation is 0.19. Its chemical composition differs from the rest of previous low calcareous groups due to its very low CaO values (< 0.7%), which also characterise individual CLI043 with whose group CLI-D is related in the dendrogram. However, individual CLI043 presents higher values in Pb and CaO.

Finally, the chemical compositions of three other loners are of interest. On the one hand, calcareous individuals CLI057 and CLI051 cannot be linked to the defined chemical groups. The first case presents higher CaO and lower values of Fe_2O_3 and Al_2O_3; differences that increase in CLI051 with even lower values for Pb and V (Table 3). Moreover, as it will be discussed in the next section, concentrations of Na_2O, K_2O and Rb in CLI051 result from alteration processes undergone during burial. On the other hand, sample CLI039 differs from the rest of the low calcareous individuals, especially in its high content of Ba and Pb, and lower concentrations of K_2O (Table 3).

(Table.3)

3.2 Mineralogical and microstructural analysis

Chemical characterisation reveals a division between individuals with calcareous (5%- 6% < CaO < 15% - 25%) and low calcareous clays (CaO < 5% -6 %) respectively, which implies a marked technical difference between such products. The results from XRD and SEM complete the information on the mineral phases and microstructures and serve as the basis for estimating their equivalent firing temperature (EFT) (Roberts 1963; Picon 1973; Tite et al. 1982; Heimann and Maggetti 2014; Gliozzo 2020).

Regarding calcareous groups CLI-A1 and CLI-A2, 13 out of 29 of the individuals in group CLI-A1 and 5 out of 8 in group CLI-A2 exhibit low EFT with the presence of chlorite/smectite clays and dolomite, which suggests an EFT below 700 °C, a temperature at which these minerals should be thermally decomposed. The identification of these phases is not always straightforward, and their peaks are usually of low intensity. Thus, one cannot exclude the possibility that they could be not identified when present in too low concentrations. The individuals presenting these phases are classified in XRD fabrics 1 to 3 for CLI-A1 and 1 to 2 for CLI-A2 (Table 4). SEM observations confirm the low EFT estimation. Individuals in these XRD fabrics exhibit microstructures with a sintering stage of no vitrification (NV) pointing to EFT below 800 °C (Fig. 7a). The presence of hematite in these samples confirms its primary phase nature (as in the low calcareous ones).

Individuals in XRD fabrics 4 (group CLI-A1; n = 8) and 3 (group CLI-A2; n = 2) do not exhibit chlorite/smectite or dolomite. Nevertheless, they also do not exhibit any firing phases. The microstructures, however, present evidence of sintering with the development of densification of the matrix with the characteristic cellular microstructure of the calcareous ceramics (Vc-/Vc) (Fig. 7b), in some cases at its initial stage (IV). This continuous vitrification stage appears at EFTs over 800 °C and is

maintained until it reaches 1050 °C. Nevertheless, the lack of firing phases enables us to estimate the EFT in the range 750/800-850 °C. Finally, individuals in XRD fabrics 5 (group CLI-A1; n = 8) and 4 (group CLI-A2; n = 1) exhibit the presence of firing phases (pyroxene and gehlenite) as well as a sintering stage of continuous vitrification (Vc) (Fig. 7c). The estimated EFT is in the range of 850-950 °C, because of the presence of illite-muscovite. The presence of calcite in those individuals can refer to relicts of primary calcite or, to some extent, the presence of secondary calcite, as confirmed by petrography, whether or not its crystallisation implies an enrichment with allochthonous calcium (Buxeda i Garrigós and Cau 1995; Cau et al. 2002). The same applies for the rest of calcareous ceramics, but also to those with low calcareous content. The individuals of CLI-B group show estimated ETF in the upper range of the previous groups - one individual in the range of 700-800/850 °C (XRD fabric 1), and two between 850-950 ºC (XRD fabric 2), although the limited number of individuals of this group must be considered.

Finally, the outlier individual CLI057 does not exhibit firing phases, neither chlorite/smectite nor dolomite. Without SEM observations for this individual the estimated EFT is in the range of 700-800/850 °C. Regarding the individual CLI051, present an estimated EFT exceptionally high for the data set in the range of 950/1000-1050 ºC with significant peaks of gehlenite and diopside, besides the possible complete decomposition of illite-muscovite. This range, for calcareous ceramics, can be considered as a non-severe overfiring. At this stage, it is common to observe that these ceramics have undergone a double process of alteration that possibly implies, in a first step, the alteration of the glassy phase developed at this stage. This alteration typically enables the lixiviation of potassium and rubidium that are thus depleted in these ceramics. In a second step, on the altered glassy phase, an authigenic sodic zeolite, analcime ($Na(AlSi_2O_6) \cdot H_2O$), crystallises incorporating allochthonous sodium enriching its initial concentration (Buxeda i Garrigós 1999; Buxeda i Garrigós et al. 2002; Schwedt et al. 2006). Indeed, individual CLI051 exhibits clear peaks of analcime by XRD (Table 4) and the highest concentration of Na_2O and the lowest of K_2O and Rb for the studied assemblage (Table 3). Thus, the actual chemical concentrations for these elements in this individual could be the result of such alteration processes.

In clear contrast to the calcareous ceramics, results of XRD and SEM relative to chemical groups CLI-C1, CLI-C2 and CLI-D exhibit low EFT, without evidence of vitrification (Figs. 7e - 7f) (Table 4). By XRD, we observe two different ranges, according to the presence or absence of chlorite/smectite phyllosilicates, which indicate an EFT lower or higher than 700 ºC. Noticeably, none of the low calcareous individuals exhibits dolomite, something that can contribute to the general lower concentrations of MgO in these low calcareous ceramics. Thus, this lower EFT range is attributed to the 3 individuals in group CLI-C1, 5 in group CLI-C2 (XRD fabrics 1 and 2) and 2 individuals in group CLI-D (XRD fabric 1). Besides, the same estimate pertains to the two low calcareous loners. Only three individuals are classified in the higher range: 2 individuals from group CLI-C2 (XRD fabric 3) and 1 individual in group CLI-D (XRD fabric 2). In those cases, chlorite/smectite has not been observed, but nor has any mineral that can be attributed to a firing phase. Moreover, these individuals, by SEM, exhibit a 'no vitrification' stage. Thus, the estimated EFT must then be <750 ºC. It should be pointed out that in group CLI-C2, sample CLI042 (XRD fabric 1) exhibits a peak at 7.59 Å (11.65°2θ) that seems to correspond to the $d_{(003)}$ peak of hydrotalcite (JCPDS #01-089-0460; $(Mg_{0.667}Al_{0.333})(OH)_2(CO_3)_{0.167}(H_2O)_{0.5}$). This mineral decomposes at very low temperatures in two steps at 300 ºC and 400 ºC, with simultaneous dehydroxylation and decarbonation (Palmer et al. 2009). Its presence, thus, must be interpreted as a secondary phase, but previously it has only been reported as a secondary phase in ceramics buried in seawater in oxic environments (Lemoine et al. 1981; Pradell et al. 1996; Amadori et al. 2002; Buxeda i Garrigós et al. 2005). Crystallisation of hydrotalcite in the previous cited studies has been linked to the enrichment with allochthonous magnesium from seawater. In the present case, the

MgO content of individual CLI042 is not abnormally high for the CLI-C2 group. At present little can be said about the mechanism of its crystallisation, or its implications in terms of perturbation of the initial chemical composition. However, it is known that in certain conditions in an alkaline environment, hydrotalcite can form after the alteration of Mg-montmorillonite (a member of the smectite group) (Cuevas et al. 2018).

(Table.4)

A final issue to discuss is the Sr content in some calcareous and low calcareous individuals. Because of these significant abnormal variations in strontium concentrations, we have excluded this element for the statistical data treatment, but at this point, it is worth considering this problem. Sr concentrations in this data set show a clear bimodal tendency with approximately 150 µg/g for low calcareous individuals and 500 µg/g for calcareous ones. Clear deviations from these values are observed in all groups but one (Table 1): CLI-A1 (CLI027, 741 µg/g; CLI033, 753 µg/g), CLI-A2 (CLI058, 801 µg/g; CLI031, 837 µg/g; CLI055, 1251 µg/g), CLI-B (CLI030, 990 µg/g; CLI024, 1167 µg/g), CLI-C1 (CLI050, 410 µg/g), CLI-C2 (CLI047, 533 µg/g). Enrichment of Sr has been previously observed in archaeological ceramics (see, for example, Picon 1987, 1991; Buxeda i Garrigós 1999). The present study has enabled the observation, by SEM, of celestine ($SrSO_4$) authigenic crystals in pores and voids (Fig. 7d). The crystallisation of this secondary phase could explain the observed enrichment of strontium. Celestine is one end member of a solid solution with barite ($BaSO_4$). Although large deposits of celestine, related to coastal marine carbonate and evaporites sequences, are rare, small deposits can be found in different sedimentary and igneous environments (Forjanes et al. 2020), such as those located at several points in the nearby pre-coastal sierras of Lorca (Manteca et al. 2005; Morales et al. 2019).

Contrariwise, barite has a much broader geological distribution than celestine, but rarely occurs in the large deposits characteristic of celestine. Even if forming a solid solution, both minerals have very different solubilities, and celestine is around 100 times more soluble than barite. In practice, this means that to precipitate strontium-rich solid solutions, the aqueous phase must be extremely poor in Ba^{2+} (Prieto et al. 1997). Thus, the presence of celestine implies the existence of an aqueous phase rich in Sr^{2+} and extremely poor in Ba^{2+} and sulfate-rich fluids, possibly by the dissolution of gypsum ($CaSO_4 \cdot 2H_2O$) or anhydrite ($CaSO_4$) (Forjanes et al. 2020). As shown in Tables 2 and 3, there is no relation between the presence of high strontium (i.e., celestine crystallisation?) and ceramic class. However, it is of interest that all calcareous individuals correspond to ceramics at the upper part of the EFT range, in which they have developed a cellular microstructure favouring a network of open porosity. This result confirms previous observations (Picon 1987, 1991; Buxeda i Garrigós 1999), although it has also been identified high strontium on low calcareous cooking pots CLI047 and CLI050 at the lower EFT range. In all cases, the affected individuals were retrieved in archaeological levels of Phase IV and mainly Phase V (Table 1). These levels are located closest to the surface within the stratigraphic sequence, something that may have favoured the precipitation of strontium and the crystallisation of celestine.

(Fig.7)

3.3 Petrographic analysis

Thin section analysis under the polarising microscope allowed the differentiation of two main petrographic fabrics and two samples that could not be assigned to the previous clusters, defined as loners. Overall, the assemblage in thin section presents a simple picture which broadly differentiates the calcareous and low-calcareous vessels.

Fabric 1: fine clay with low-grade metamorphic rocks and grog temper.

This group is quite homogeneous in terms of petrographic composition and textural parameters.

Almost all calcareous individuals from Castellar de Librilla have been included in this group, as well as the non-calcareous individual CLI035. It is a heterogeneous ceramic assemblage (n = 41) that contains individuals from phases Lib-II to Lib-V, with wheel-made vessels that comprise burnished grey ceramics, red slip ware and amphorae, as well as handmade triangular supports and the Late Bronze Age burnished plate (Fig. 5, Table 4).

Fabric 1 is characterised by a fine Neogene clay groundmass containing common, poorly sorted low-grade metamorphic rocks and added grog temper (Fig. 8). The grain-size of the aplastic inclusions is generally bimodal, with a coarse fraction single to open spaced ranging from fine silt to very coarse sand. The sub-rounded inclusions are dominated by elements corresponding to low-grade regional metamorphism characterised by the appearance of quartz, white mica schist, phyllite, alkaline feldspar and calcite; the presence of nematoblastic and granoblastic textures was frequently observed. Coarse aplastic inclusions of this fabric also comprise opaque minerals and grog temper that, sometimes, reach significant sizes. The voids are meso and macro rounded and elongated, and some individuals present secondary calcite. The matrix is calcareous, dark brown to black in PPL, with some variation between the inner and outer surfaces, contains single to open space quartz, mica, muscovite and biotite. There are also rare small microfossils, including foraminifera and ostracods.

Three sub-groups may be distinguished according to the frequency or presence of specific inclusions and to the characteristics of the matrix. The features mentioned above distinguish Fabric 1.1 (n = 31), the most frequent (Figs. 8a - 8d). Fabric 1.2 (n = 8) presents the same type of aplastic inclusions, but fewer and smaller (Figs. 8e - 8g). Besides, its groundmass exhibits colours from the dark red plate or brown in PPL to very dark brown/black in XP. Fabric 1.3 (sample CLI055) differs only by it containing a single sub-angular, coarse sand conglomerate (Fig. 8h).

Fabric 2: frequent, very coarse and low-grade metamorphic rocks with grog temper.

Fabric 2 (Fig. 5, Table 4) presents a homogeneous matrix in terms of its aplastic inclusions and groundmass. Macroscopically, all group members (n = 13) are handmade cooking pots from phases Lib-II to Lib-V, perhaps some of which may have been used for storage. The pots examined are globular in shape, with a short, rounded rim, some with small handles; the surfaces are often barely finished or just smoothed, with black and dark brown surfaces that have abundant visible aplastic inclusions.

Fabric 2 is dominated by frequent, poorly sorted, very coarse low grade metamorphic rocks and grog temper (Figs. 9.a - 9.d). The aplastic inclusions are bimodal in grain-size and single to double spaced. The coarse fraction, from fine silt to rounded and sub-rounded granules, is composed of metamorphic rocks, mainly mica schists and phyllites with nematoblastic and granoblastic textures and added grog temper. Other inclusions include quartz, and less frequent alkaline feldspar and opaque minerals. The matrix voids present a meso and macro size (0.5 – 2 mm) with an elongated shape. The clay matrix is generally low calcareous and contains single to open space quartz, feldspar, and muscovite and biotite. The colour of the groundmass is generally homogenous, brown to black colour in PPL, with some variations between the inner and outer surfaces. Due to the similarities of texture and the nature and distribution of inclusions, no sub-groups have been defined.

(Fig.8) & (Fig.9)

Other fabrics

Two individuals have unique compositions and are classified as loners, as indeed was the case with the chemistry of these two samples.

Individual CLI039 is characterised (Fig. 9e) by dominant, single-spaced, rounded granules of schist and phyllite, showing clear crenulation cleavage, in a quartz rich matrix. The coarse fraction, ranging from

medium silt to sub-rounded granules, contains inclusions of quartz, biotite, feldspars and opaque minerals; while the fine fraction present dominant quartz, and frequent muscovite and biotite.
Individual CLI051 (Fig. 9f) has a quartz rich matrix with few low-grade metamorphic rocks and added grog temper. The coarse fraction presents schist, quartz and fewer feldspar, phyllite, biotite and opaque minerals from medium silt to very coarse sand. The most significant feature of this fabric is the groundmass and the fine fraction, where there is dominant quartz and few feldspar, muscovite and biotite, with rare microfossils (foraminifera).

4. Discussion and archaeological implications

There is substantial agreement between the different analytical techniques applied to the assemblage of Castellar de Librilla. Although several clusters result from the statistical treatment of the XRF chemical data, they sub-divide rather than contradict the broad division of the assemblage by the petrographic study, even being in agreement on some outlying loner samples. XRF and petrography indicate that, despite significant typological variability in the assemblage and two main choices of raw materials, the two main groups of the assemblage are of a similar provenance, compatible with the area of their findspot. Some of the detail of variability might be expected in an assemblage which spans the second half of the 8th century to the early 5th century BC. But this does not obscure the consistent picture.

The low calcareous samples, essentially the handmade ceramics, including cooking pots and the LBA burnished plate, are divided into three groups based on their chemical composition. CLI-C1, CLI-C2 and CLI-D. Despite differences represented in the dendrogram (Fig. 5) and the PCA (Fig. 6), the clay matrices of these handmade cooking pots (including loner CLI043) are grouped in thin section as Fabric 2. Sample CLI039, is considered on the ground of both chemistry and petrography to have a rather different provenance from the other low calcareous samples. The presence in CLI-C1, CLI-C2 and CLI-D groups of coarse, low-grade metamorphic rocks are compatible with a local provenance, and specifically the geological characteristics of Castellar de Librilla environment. Moreover, individual CLI046, classed in group CLI-C2, was recovered in the kiln dump.

These clear analytical results testify to the local production of low fired (consistently below 750 °C) handmade ceramics in the surroundings of the settlement that endured from the last period of the Late Bronze Age into the Iron Age. Its typological forms, forming techniques, clay recipes and other details of technology are characterised by a marked continuity up to the transition to the Iberian culture. In ceramic terms, it comprises a survival that stands out amid a cultural ambience where not only do wheel-made ceramics appear through contacts with the Phoenicians, but the autochthonous workshops begin to manufacture their own ceramics made on the wheel. Handmade cooking pots seems to have been the forms most resistant to change in this period, perhaps suggesting a continuity of Late Bronze Age dietary and commensal practices, revealing somewhat conservative choices by both consumers and the producers of cooking vessels. The maintenance of these commensal and technological practices, both activities embedded in daily social life, suggests a deliberate preservation of communal identity which dates from the Late Bronze Age (Delgado 2010).

If the non-calcareous samples illustrate the importance of local productions and their persistence throughout the different phases of settlement, the calcareous ceramics suggest the same consideration. The dendrogram resulting from statistical treatment of XRF data shows the presence of two main clusters, CLI-

A and CLI-B. The majority of the calcareous individuals, including five individuals recovered from the combustion chamber of the pottery kiln (CLI023, 33, 56, 55, and 58), has been grouped within CLI-A1 and CLI-A2 clusters, which presents a very low chemical variability that stands out despite the typological diversity and the ceramic classes that have been included: grey pottery, red slipware, red common ware, amphorae, handmade pots and triangular supports. The homogeneity of this monogenic group is also clear in thin section, given that all the individuals are assigned to Fabric 1 - including the 6 individuals that have not been analysed by XRF and XRD -, except for the handmade samples CLI048 and CLI049. The only exception to this pattern is that cluster CLI-B includes three table ware samples differentiated by higher MgO values, but whose clay matrix and aplastic inclusions link it to Fabric 1, as also in the case of the loner CLI057. These petrographic similarities could also point to a local origin for this chemical group CLI-B, an argument that would be reinforced by sample CLI024 from the dump associated with the pottery kiln (Table 1).

Despite the typological heterogeneity of the ceramic assemblage, Fabric Group 1 is characterised by a fine clay matrix with few aplastic components, distinctive of geological environments rich in sedimentary and Neogene materials, common in the landscape surrounding the settlement. The coarse inclusions are more disaggregated than in Fabric 2, although typical elements of low-grade regional metamorphism, such as quartz, mica schist and phyllite, are still clear. These metamorphic materials are documented in the geological strata of the lower part of Sierra del Castellar de Librilla due to their formation on the Alhama de Murcia fault, so a local origin may be proposed for these products. In addition, a large conglomerate inclusion has been documented on the clay matrix of sample CLI055 that agrees with the geological composition from the nearby Sierra de la Muela.

The shared characteristics of Fabric 1 and 2 not only suggest a similar geological area, but a common provenance. The classification of handmade samples CLI048 and CLI049 defined by XRF as calcareous individuals and assigned to Fabric 2 and the non-calcareous CLI035 sample attached to Fabric 1, allow us to propose a close relationship between both repertoires. Therefore, these crossover results point to a common provenance that may be geologically compatible with the geological characteristics of the Rambla de Algeciras environment. In this way, it is possible that in the area associated with the main settlement of Castellar de Librilla, one or several workshops used geologically similar clays, perhaps from different outcrops.

The examination of the microstructures by SEM and the XRD analysis of handmade ceramics show a lack of vitrification and firing phases (Fig. 7; Table 4), indicating low or very low firing temperatures (< 750 ºC) for all these cooking pots dated up to the beginning of the 5th century BC. These very low firing temperatures may indicate open firing, continuing the pottery strategies of Late Bronze Age, even while pottery kilns were already in use in the site.

Firing of the wheel-made pottery seems to be rather different. No specific pattern has been detected that associates EFTs with certain productions or chronological phases, and the results show a wide variety of firing temperatures from very low to those with vitrified clays (850-950 ºC), across all ceramic classes and chronological phases. These differences in EFT could be due to the position each object occupied in the upper chamber of the kiln during firing, as well as reflecting problems in reaching firing temperatures high enough to develop sintering to the stage of continuous vitrification (800/850 ºC - 1050 ºC). While such

a wide range of tolerance in calcareous ceramics over which vitrification would be achieved is beneficial to potters, the range of temperatures implies a relatively poor control. The only exceptions are the calcareous hand-made triangular supports of kiln furniture, all of which exhibit a sintering stage of continuous vitrification, and in individual CLI051 EFT is of non-severe overfiring (with the presence of secondary analcime). These, however, are not directly compatible, as they are not pottery vessels and most likely are subjected to several firing episodes in their use life.

Overall, the analytical programme allows us to define and characterise the local products of Castellar de Librilla; an origin which, on the other hand, is reinforced as some of the ceramics under analysis are directly related to the potter's kiln. It demonstrates not only the existence of a pottery tradition maintained from Late Bronze Age and consolidated for almost three centuries, but also the beginning of wheel-made ceramic production in the workshop or workshops of the settlement from a very early in the period of Phoenician contact. In this sense, the trend to the consumption of grey pottery, red slipware, and amphorae led to the use of double-chamber kilns which were capable of more stable firing conditions. These pottery types and innovative kiln designs seem to have been adopted by potters from Castellar de Librilla already in the 8th century, even before the excavated kiln known to us, which is dated to the 6th century BC.

Clearly, the nature of the transmission of technological practice, through everyday craft practice, implies that these technological changes involved the influence of Phoenician potters on the local craftspeople, especially in the case of the adoption of the double-chamber kiln. After all, to become an expert potter, many years of intensive practice are needed (Roux and Corbetta 1989) and within an apprenticeship that takes place from an early age in the framework of a workshop and under the supervision of mentors, whose lineage and craft tradition is joined by apprentices (Ingold 2001). In the context of the Iberian Southeast, the technological development of local potteries involved not only the adoption of the wheel, but complex structures and know-how involved in kiln firing.

This was undoubtedly part of a more general technological transmission, as potters' kilns in autochthonous settlements across the Iberian Southeast – Cerro de los Infantes (Contreras et al. 1983), Calañas de Marmolejo (Molinos et al. 1994), Lorca (Martínez 2006), Castellar de Librilla (Ros 1989) – follow the same prototypes located in some Phoenician colonies such as Cerro del Villar (Aubet et al. 1999) and Málaga (Arancibia and Escalante 2006). All Iberian cases involve kilns with a circular plan and solid central pillar to support the grill, structures based on models from further East, such as those identified in Sarepta (Anderson 1987) or Akko (Dothan, 1989).

However, the installation of these foreign artisans did not imply a drastic change in the consumption patterns of ceramics by local communities, nor did it mean the disappearance of the autochthonous potters. The survival of an important part of traditional Late Bronze Age repertoires and the persistence of hand-made manufacturing tradition suggest a co-existence or even a hybrid ambiance, as a result of intercultural encounters of potters. Although mixed ceramic repertoires clearly developed, this process was conditioned by a phenomenon of selective incorporation, through which the autochthonous communities decide what to accept and what to reject. This agency of the Early Iron Age groups becomes evident, in some cases adapting the inherited material culture and practice to the new means of production or in others maintaining their ceramic tradition.

(Fig.10) & (Fig.11)

In this way, a mixed or hybrid assemblage in which handmade and wheel-made individuals shared spaces and functionalities was finally configured (Fig. 10). However, this material dichotomy was only possible based on the consumption patterns of the autochthonous communities, constituting a generalised phenomenon across this and other hilltop centres of the region, such as Peña Negra or Santa Catalina (González Prats 1983; Ros 1986-1987), and in rural sites like Los Saladares, Torre de Sancho Manuel or Cabezo Ventura (Arteaga and Serna 1975; Cutillas 2019). Itself conditioned by the development of these internal demands, the evolution of the autochthonous pottery workshops occurred in parallel to that of society itself, adapting their products to internal demand to be able to sell them and guarantee their own subsistence. For this reason, a mixed production by local workshops has been proposed, with the manufacture of wheel-made ceramics for the table, storage and transport, and handmade ceramics that maintain their presence among cooking wares and table repertoires.

The hypothesised intrusive potters seem to have had to respond to the internal demands of the communities in which they were installed, adapting their own products and technological practice to a cultural environment still profoundly rooted in the Late Bronze Age traditions. In this way, their identities would be diluted and mixed with the local groups. At the same time, techniques and knowledge were assimilated and reproduced by the next generation of artisans under a cross-cultural paradigm resulting from the intercultural encounter that characterises the first part of the 1st millennium BC. However, despite the technological changes experienced, the Early Iron Age identities were not eclipsed. This cultural resistance to change explains the commitment to certain habits, gestures and vessels linked to the Late Bronze Age tradition, also suggesting the survival of traditional ways of cooking and the associated diets.

5. Conclusions

This first integrated analytical programme (XRF, XRD, petrography, SEM) has produced clear insight into the ceramic repertoires of Castellar de Librilla, one of the main autochthonous settlements of the Iberian Southeast. Building on detailed macroscopic studies (Ros 1989), it characterised production, and highlighted the elements of continuity and change in the pottery of the area. Distinct changes occur in pottery production from the Late Bronze Age to the beginning of the Iberian culture, a production which chemistry and petrography clearly indicates took place within the area of Castellar de Librilla. The different types of pottery produced there encompass two markedly different technological sequences and sets of knowledge, and we have established that this co-existence of different technologies, perhaps different communities of practice, start at least as early as the second half of the 8th century BC. This new date is key to understanding the mechanisms of change at play in the region's potteries and indirectly demonstrates the existence of specialised workshops in Castellar de Librilla before the construction of kiln M.

The technological changes and the incorporation of new structures and tools, a consequence of contact with the Phoenician colonies, led to a pottery production in the local environment previously considered foreign, such as early grey pottery, amphorae and red slipware. In this Castellar de Librilla was not alone. On the contrary, the results show the capacities of these local potters' workshops and confirm the picture at other autochthonous workshops, such as those in Peña Negra II (González Prats and Pina 1983) and Calañas de Marmolejo (Molinos et al. 1994), and suggest that we do not have to resort to simple colonialist paradigms suggesting that the control of these technologies is limited exclusively to Phoenician potters. If the appearance of kilns was due to the arrival of Phoenician artisans or apprentices to the autochthonous

settlements, they were immersed in a new cultural ambience where the demands were different from those that occurred in the Phoenician colonies. This process of cultural resistance by the communities of the Iberian Southeast was reflected in the maintenance of certain ceramic vessels and the continuity in hand-forming of such pottery. The fact that several Late Bronze Age pottery forms were adapted for production on the wheel also highlights the hybridisation processes active in this specific material sphere.

The different processes in the ceramic sphere are active participants in many other complex phenomena beyond materiality, revealing the difficulty of viewing these communities simply as a product of a game of cultures in contact (Bhabha 1994). Our results certainly suggest the agency of the autochthonous communities, especially in the face of the supposed vertical acculturation from the Phoenician colonies, and the existence in the productive processes of behavioural chains (Schiffer 2010; Hodder 2012) that should be understood from the dynamics of the local Iberian cultural context of the Early Iron Age. The emergence of mixed assemblages that combine handmade and wheel-made pottery, manufactured in both cases by autochthonous workshops, points to the essential role that the Early Iron Age workshops developed at this Mediterranean scenario and not only at the local level. This composite picture of practice and products has value within regional and peninsular economic networks, given that the dichotomy "wheel-made ceramic = Phoenician and handmade ceramic = autochthonous", has proven to be an over-simplification. This insight suggests that the integration of an analytical approach to ceramic provenance and technological reconstruction provides real insight into economic and cultural influence along the colonial coastline, highlighting the dynamic processes involved in craft production, consumption and the building of identities.

Acknowledgements: the authors would like to thank the technical staff who have collaborated on the XRF, XRD and SEM-EDX analyses which were carried out in the Centres Científics i Tecnològics de la Universitat de Barcelona, and the thin sections prepared in the Laboratory of Geology of the University of Murcia. BCV would like to thank Veronica Testolini for facilitating his training at the University of Sheffield.

Funding: This work was made be possible by funding from the *ALAFMET: Alfarerías autóctonas y fenicias en el SE ibérico. Una mirada arqueométrica* research project supported by Fundación PALARQ and was developed in the framework of the R&D&I research project *HAR2017-85726-C2-1-P: Carthago nova: paleotopografía y evolución medioambiental del sector central del Sureste ibérico (ARQUEOTOPOS III)*, funded by the Spanish Ministry of Science and Innovation and the European Regional Development Fund (ERDF). This is also part of the activities of the Research Group on Archaeology of Complex Societies and Processes of Social Change, Universitat de Barcelona (ARQUB, GRACPE) (2017 SGR 1774).

Availability of data and material: All data needed to elaborate this work and its conclusions are present in the paper. Additional data related to this paper may be requested from the authors.

Conflict of interest: The authors declare no competing interests

6. References

Aitchison J (1986) The Statistical Analysis of Compositional Data. Chapman and Hall, London.

Albero D, Cau MA (2016) Technological choices in handmade indigenous pottery from Western Mallorca (Balearic Islands, Spain) (c. 1200-75 BC): an archaeometric approach. Archaeometry 59(4):1–25. https://doi.org/10.1111/arc.12273

Amadori ML, Baldassari R, Lanza S, Maione M, Penna A, Acquaro E (2002) Archaeometric study of Punic amphorae from the underwater recoveries of Pantelleria island (Sicily). Rev Archéométrie 26:79–91. https://doi.org/10.3406/arsci.2002.1025

Anderson WP (1987) The Kilns and Workshops of Sarepta (Sarafand, Lebanon): remnants of a Phoenician Ceramic Industry. Berytus 35:41–66

Arancibia A, Escalante MM (2006) La Málaga fenicio-púnica a la luz de los últimos hallazgos. Mainake 28:333–360.

Argus DF, Gordon RG, DeMets C (2011) Geologically current motion of 56 plates relative to the no-net-rotation reference frame. Geochemistry, Geophysics, Geosystems 12(11):1–13. https://doi.org/10.1029/2011GC003751

Arteaga O, Serna A (1975) Los Saladares-71. *Noticiario Arqueológico Hispánico* 3:7–140.

Aubet ME, Carmona P, Curià E, Delgado A, Fernández A, Párraga M (1999) Cerro del Villar I. El asentamiento fenicio en la desembocadura del río Guadalhorce y su interacción con el hinterland. Junta de Andalucía, Sevilla.

Bhabha HK (1994) The Location of Culture. Routledge, New York.

Buxeda i Garrigós J (1999) Alteration and contamination of archaeological ceramics: the perturbation problem. J Archaeol Sci 26:295–313.

Buxeda i Garrigós J (2018) Compositional Data Analysis. In: López Varela SL (ed) The Encyclopedia of Archaeological Sciences. John Wiley & Sons, Oxford, pp 1–5.

Buxeda i Garrigós J, Cau MA (1995) Identificación y significado de la calcita secundaria en cerámicas arqueológicas. Complutum 6:293–309.

Buxeda i Garrigós J, Cau MA, Madrid M, Toniolo A (2005) Roman Amphorae from the Iulia Felix Shipwreck: Alteration and Provenance. In: Hars H, Burke E (eds) Proceedings of the 33rd International Symposium on Archaeometry, 22-26 April 2002, Amsterdam. Institute for Geo- and Bioarchaeology of the Vrije Universiteit in Amsterdam, Amsterdam, pp 149–151.

Buxeda i Garrigós J, Kilikoglou V (2003) Total variation as a mesure of variability in chemical data sets. In: Zelst LV (ed) Patterns and Process. A festschrift in honor of Dr. Edward V. Sayre. Smithsonian Center for Materials Research and Education, Maryland, pp 185–198.

Buxeda i Garrigós J, Kilikoglou V, Day PM (2001) Chemical and mineralogical alterations of ceramics from a late bronze age kiln at Kommos, Crete: the effect on the formation of a reference group. Archaeometry 43:349–371. https://doi.org/10.1111/1475-4754.00021

Buxeda i Garrigós J, Madrid M (2017) Designing rigorous research: integrating Science and Archaeology. In: Hunt A (ed) The Oxford Handbook of Archaeological Ceramic Analysis. Oxford University Press, Oxford, pp 19–47.

Buxeda i Garrigós J, Mommsen H, Tsolakidou A (2002) Alterations of Na, K and Rb concentrations in Mycenaean pottery and a proposed explanation using X-ray diffraction. Archaeometry 44(2):187–198. https://doi.org/10.1111/1475-4754.t01-1-00052

Calmel-Ávila A (2000) Procesos hídricos holocenos en el Bajo Guadalentín (Murcia, España). Cuaternario y Geomorfología 14(3):65–78.

Carrión JS, Fernández S, Jiménez-Moreno G, Fauquette S, Gil-Romera G, González-Sampériz P, Finlayson C (2010) The historical origins of aridity and vegetation degradation in southeastern Spain. J Arid Environ 74(7):731–736. https://doi.org/10.1016/j.jaridenv.2008.11.014

Cau MA, Day PM, Montana G (2002) Secondary calcite in archaeological ceramics: evaluation of alteration and contamination processes by thin section study. In: Kilikoglou V, Maniatis Y, Hein A (eds) Modern trends in ancient ceramics. British Archaeological Reports, International Series 1011, Oxford, pp 9–18.

Cau MA, Fantuzzi L, Albero D, Tsantini E, García Roselló J, Calvo M (2019) Archaeometric characterisation of Iron Age indigenous pottery from the staggered turriform of Son Ferrer, Mallorca, Spain. Geoarchaeology 34:149–168. https://doi.org/10.1002/gea.21696

Contreras F, Carrión F, Jabaloy EM (1983) Un horno de alfarero protohistórico en el cerro de los Infantes (Pinos Puente, Granada). In: XVI Congreso Nacional de Arqueología. Univ. de Zaragoza, Zaragoza, pp 533–538.

Cuevas J, Ruiz AI, Fernández R, González-Santamaría D, Angulo M, Ortega A, Torres E, Turrero MJ (2018) Authigenic Clay Minerals from Interface Reactions of Concrete-Clay Engineered Barriers: A New Perspective on Mg-Clays Formation in Alkaline Environments. Minerals 8 (362):1–18. https://doi.org/10.3390/min8090362

Cutillas B (2019) El ajuar cerámico de una unidad rural del Hierro Antiguo: el caso de La Torre de Sancho Manuel (Lorca, R. de Murcia). In: Coll J (ed) Opera Fictiles. Estudios transversales sobre cerámicas antiguas de la península ibérica. SECAH-La Ergástula, Valencia, pp 11–26.

Cutillas B, Ros MM (2020) Asentamientos polinucleares y resiliencia urbana entre el Bronce Final y la Edad del Hierro en el Sureste ibérico: nuevos datos a partir del Castellar de Librilla. Complutum 31(1):71–96. https://doi.org/10.5209/cmpl.71650

Delgado A (2010) De las cocinas coloniales y otras historias silenciadas: domesticidad, subalternidad e hibridación en las colonias fenicias occidentales. In: Mata C, Pérez G, Vives-Ferrándiz J (eds) De la Cuina a la Taula. IV Reunió d'Economia en el Primer Millenni a.C. Sagvntvm Extra 9, Valencia, pp 27–42.

Dothan M (1989) Archaeological evidence for movements of the early "Sea Peoples" in Canaan. In: Gitin S, Dever WG (eds) Recent excavations in Israel: Studies in Iron Age archaeology. Eisenbrauns, Winona Lake, pp 59–70.

Egozcue JJ, Pawlowsky-Glahn V (2011) Basic concepts and procedures. In: Pawlowsky-Glahn V, Buccianti A (eds.) Compositional Data Analysis. Theory and Applications. Wiley, Chichester, pp 12–28.

Fernández A, Rodríguez A (2007) Tartessos desvelado. La colonización fenicia del Suroeste peninsular y el origen y ocaso de Tartessos. Almuzara, Córdoba.

Forjanes P, Astilleros JM, Fernández-Díaz L (2020) The Formation of Barite and Celestite through the Replacement of Gypsum. Minerals 10(189): 1–17. https://doi.org/10.3390/min10020189

García Blánquez LA (1996) El Cerro de la Fuente del Murtal, Alhama de Murcia (1ª campaña 1991): poblado fortificado del período de transición Bronce Final / Hierro Antiguo en el eje de poblamiento Segura-Guadalentín (Murcia). Memorias de Arqueología de la Región de Murcia 5:65–85.

García Menárguez A, Prados, F (2014) La presencia fenicia en la Península Ibérica: el Cabezo Pequeño del Estaño (Guardamar del Segura, Alicante). Trabajos de Prehistoria 71(1):113–133. https://doi.org/10.3989/tp.2014.12127

Gliozzo E (2020) Ceramic technology. How to reconstruct the firing process. Archaeol Anthropol Sci 12:1–24. https://doi.org/10.1007/s12520-020-01132-z

González Prats A (1983) Estudio Arqueológico del poblamiento antiguo de la Sierra de Crevillente (Alicante). Univ. de Alicante, Alicante.

González Prats A (2011) La Fonteta. Excavaciones de 1996-2002 en la colonia fenicia de la actual desembocadura del río Segura (Guardamar del Segura, Alicante). Univ. de Alicante, Alicante.

González Prats A, Pina JA (1983) Análisis de las pastas cerámicas de vasos hechos a torno de la fase orientalizante de Peña Negra (675-550/535 a.C.). Lucentum 2:115–146. https://doi.org/10.14198/lucentum1983.2.06

Heimann RB, Maggetti M (2014) Ancient and Historical Ceramics. Materials, Technology, Art, and Culinary Traditions. Schweizerbart Science Publishers, Stuttgart.

Herrero P, Álvarez JA, Martínez JJ (2017) Análisis estructural en el segmento Alhama de Murcia - Alcantarilla (Falla de Alhama de Murcia) y sus implicaciones en la peligrosidad sísmica. Geogaceta 62:11–14.

Hodder I (2012) Entangled: an Archaeology of the Relationships between Humans and Things. Wiley-Blackwell, Malden.

Ingold T (2001) Beyond art and technology: the anthropology of skill. In: Schiffer MB (ed) Anthropological perspectives on technology. University of New Mexico Press, Albuquerque, pp 17–31.

Kampschuur W, Langeberg CW, Montenat CH, Pignatelli R, Egeler CG (1972) *Mapa Geológico de España. Escala 1:50.000 hoja 933 (Alcantarilla)*. IGME, Madrid.

Lemoine C, Poupet P, Barrandon JN, Borderie B, Meille E (1981) Étude de quelques altérations de composition chimique des céramiques en milieu marin et Terrestre. Rev Archéométrie 1:349–360. https://doi.org/10.3406/arsci.1981.1166

Lomba J, Cano M (2002) El Cabezo de la Fuente del Murtal (Alhama): Definición e interpretación de una fortificación de finales del siglo VII a.C. e inicios del VI en la rambla de Algeciras (Alhama de Murcia, Murcia). Memorias de Arqueología de la Región de Murcia 11:165–204.

Lorrio A, Pernas S, Torres M (2016) Puntas de flecha orientalizantes en contextos urbanos del Sureste de la Península Ibérica: Peña Negra, La Fonteta y Meca. CuPAUAM 42:9–78. https://doi.org/10.15366/cupauam2016.42.001

Manteca JI, Pérez MA, López MA (2005) La Industria Minera en Murcia durante la época contemporánea. Bocamina 15:123–136.

Martín-Fernández JA, Buxeda i Garrigós J, Pawlowsky-Glahn V (2015) Logratio Analysis in Archaeometry: Principles and Methods. In: Barceló JA, Bogdanovic I (eds) Mathematics and Archaeology. CRC Press, Boca Ratón, pp 178–189.

Martínez M (2006) Excavación arqueológica en la zona de La Alberca (Lorca, Murcia). Un horno alfarero de los siglos VII-VI a.C. y un centro comercial y militar de época tardopúnica y romana. Memorias de Arqueología de la Región de Murcia 14:213–260.

Molinos M, Rísquez C, Serrano JL, Montilla S (1994) Un problema de fronteras en la periferia de Tartessos: Las Calañas de Marmolejo (Jaén). Univ. de Jaén, Jaén.

Morales ML, López G, López A (2019) El yacimiento de azufre de La Serrata, Lorca, Murcia. Paragénesis 2:47–58.

Navarro F, Ros MM, Rodríguez T, García J, Fierro E, Carrión J, Flores JA, Bárcenas MA, García MS (2014) Evaporite evidence of a mid-Holocene (c. 4550-4400 cal. BP) aridity crisis in southwestern Europe and palaeoenvironmental consequences. Holocene 24:489–205. https://doi.org/10.1177/0959683613520260

Nijboer AJ, van der Plicht J (2006) An interpretation of the radiocarbon determinations of the oldest indigenous-Phoenician stratum thus far, excavated at Huelva, Tartessos (south-west Spain). Bulletin des Antieke Beschaaving 81:31–36. https://doi.org/10.2143/BAB.81.0.2014423

Palmer SJ, Spratt HJ, Frost RL (2009) Thermal decomposition of hydrotalcites with variable cationic ratios. J Therm Anal Calorim 95(1):123–129. https://doi.org/10.1007/s10973-008-8992-4

Picon M (1973) Introduction à l'étude technique des céramiques sigillées de Lezoux. Unversité de Dijon, Dijon.

Picon M (1987) La fixation du baryum et du strontium par les céramiques. Rev Archéométrie 11:41–47. https://doi.org/10.3406/arsci.1987.1236

Picon M (1991) Quelques observations complémentaires sur les altérations de composition des céramiques au cours du temps: cas de quelques alcalins et alcalino-terreux. Rev Archéométrie 15:117–122. https://doi.org/10.3406/arsci.1991.1263

Pradell T, Vendrell-Saz M, Krumbein W, Picon M (1996) Altérations de céramiques en millieu marin: les amphores de l'épave romaine de la Madrague de Giens (Var). Rev Archéométrie 20:47–56. https://doi.org/10.3406/arsci.1996.936

Prieto M, Fernandez-Gonzalez A, Putnis A, Fernandez-Diaz L (1997) Nucleation, growth, and zoning phenomena in crystallizing (Ba,Sr)CO_3, Ba(SO_4,CrO_4), (Ba,Sr)SO_4, and (Cd,Ca)CO_3 solid solutions from aqueous solutions. Geochimica et Cosmochimica Acta 61(16):3383–3397. https://doi.org/10.1016/S0016-7037(97)00160-9

Quinn P (2013) Ceramic petrography. The interpretation of archaeological pottery and related artefacts in thin section. Archaeopress, Oxford.

R Core Team (2021) R: A Language and Environment for Statistical Computing. R Foundation for Statistical Computing, Vienna. http://www.R-project.org/

Roberts J (1963) Determination of the firing temperature of ancient ceramics by measurement of thermal expansion. Archaeometry 6:21–25. https://doi.org/10.1111/j.1475-4754.1969.tb00636.x

Ros MM (1986-1987) El poblado de Santa Catalina del Monte: una aproximación a la urbanística del siglo VI a.C. en el ámbito territorial del eje Segura-Guadalentín. Cuadernos de Prehistoria y Arqueología 13-14:77–88.

Ros MM (1989) Dinámica urbanística y cultura material del Hierro Antiguo en el Valle del Guadalentín. Univ. de Murcia, Murcia.

Ros MM (2017) Nuevos datos en torno a la presencia fenicia en la Bahía de Mazarrón (Sureste Ibérico). In: Prados F, Sala F (eds.) El Oriente de Occidente. Fenicios y púnicos en el área ibérica. Univ. de Alicante, Alicante, pp 79–104.

Rouillard P, Gailledrat E, Sala F (2007) L'établissement protohistorique de La Fonteta (fin VIIIe – VIe siècle av. J.-C.). Casa de Velázquez, Madrid.

Roux V, Corbetta D (1989) Wheel-throwing technique and craft specialisation. In Roux V (ed.) The 'Potter's wheel. Craft specialisation and technical competence. Oxford - IBH Publishing, New Delhi, pp 1–91.

Sánchez V, Galindo L, Juzgado M, Dumas M (2011) La desembocadura del Guadalhorce en los siglos IX y VIII a.C. y su relación con el Mediterráneo. In: Domínguez JC (ed) Gadir y el círculo del Estrecho revisados. Propuestas de la arqueología desde un enfoque social. Univ. de Cádiz, Cádiz, pp 187–197.

Schwedt A, Mommsen H, Zacharias N, Buxeda i Garrigós J (2006) Analcime crystallisation and compositional profiles—comparing approaches to detect post-depositional alterations in archaeological pottery. Archaeometry 48 (2):237–251. https://doi.org/10.1111/j.1475-4754.2006.00254.x

Schiffer M (2010) Behavioral Archaeology. Principles and Practice. Equinox, London-Oakville.

Tite MS, Maniatis Y, Meeks ND, Bimson M, Hughes MJ, Leppard SC (1982) Technological Studies of Ancient Ceramics from the Near East, Aegean and Southeast Europe. In: Wertime TA, Wertime SF (eds) The evolution of the first fire-using industries. Smithsonian Institution Press, Washington, pp 61–71.

van de Boogaart KG, Tolosana-Delgado R (2013) Analysing Compositional Data with R. Springer-Verlag, Berlin.

van Dommelen P (1998) On colonial grounds: a comparative study of colonialism and rural settlement in first millennium BC west central Sardinia. University of Leiden, Leiden.

Whitbread IK (1989) A proposal for the systematic description of thin sections towards the study of ancient technology. In: Maniatis Y (ed) Archaeometry Proceedings of the 25th International Symposium (Held in Athens from 19 to 23 May 1986). Elsevier, Amsterdam, pp 127–138.

Whitbread IK (1995) Greek transport amphorae. A petrological and archaeological study. British School at Athens, Athens.

Phase	Methods	Wheelmade (42)							Handmade (21)			Total
		Grey pottery (21)			Red slip ware (11)		Red common ware (1)	Transport ware (9)	Burnished LBA (1)	Cooking ware (16)	Furniture ware (4)	
		Plate	Close plate	Round support	Plate	Jar	Lamp	Amphora	Plate	Cooking pot	Triangular support	
II (end 8th cent. BC)	XRF-XRD-OM	CLI001*, 2* (**2**)							CLI035 (**1**)	CLI036 (**1**)	CLI038 (**1**)	8
	XRF-XRD									CLI037 (**1**)		
	OM							CLI063, 64 (**2**)				
III (7th cent. BC)	XRF-XRD-OM	CLI007, 8, 9, 10, 11*, 12 (**6**)			CLI003*, 4, 5* (**3**)					CLI039, 40, 41, 42, 43 (**5**)	CLI044 (**1**)	18
	XRF-XRD				CLI006 (**1**)							
	OM							CLI061, 62 (**2**)				
IV (6th cent. BC)	XRF-XRD-OM	CLI018, 20, 23*K (**3**)		CLI019 (**1**)	CLI013, 14, 15* (**3**)		CLI017 (**1**)			CLI045*, 46*D, 48, 49, 50 (**5**)	CLI051 (**1**)	19
	XRF-XRD	CLI021 (**1**)	CLI022 (**1**)							CLI047 (**1**)		
	OM							CLI059K, 60K (**2**)				
V (end 6th/5th cent. BC)	XRF-XRD-OM	CLI028, 30, 32, 33*K, 34* (**5**)	CLI031* (**1**)	CLI0029 (**1**)	CLI024*D (**1**)	CLI027 (**1**)		CLI056K, 57, 58*K (**3**)		CLI052, 53*, 54 (**3**)	CLI055K (**1**)	18
	XRF-XRD				CLI025, 26 (**2**)							
	OM											
Total		17	2	2	10	1	1	9	1	16	4	63

* Individual observed by SEM (n = 15)

XRF-XRD-OM (n = 50), XRF-XRD (n = 7), OM (n = 6)

K Individuals recovered from stratigraphic units related to the combustion chamber of the pottery kiln (n = 7).

D Individuals recovered from the dump of the pottery kiln (n = 2).

Table 1. List of analysed samples from Castellar de Librilla. In red: individuals with high Sr concentrations

	Na_2O	MgO	Al_2O_3	SiO_2	P_2O_5	K_2O	CaO	TiO_2	V	Cr	MnO	Fe_2O_3	Co	Ni	Cu	Zn	Ga	Rb	Sr	Y	Zr	Nb	Mo	Sn	Ba	Ce	W	Pb	Th	LOI
CLI001	0.77	2.20	14.98	51.27	0.18	3.67	11.85	0.67	108	87	0.03	5.87	27	33	14	60	18	109	359	24	174	18	2	3	346	65	79	20	15	9.02
CLI002	0.86	2.42	13.16	42.45	0.20	3.33	16.24	0.56	94	71	0.04	5.39	21	32	17	80	16	84	463	20	138	15	2	2	270	52	16	27	14	16.64
CLI003	0.76	2.42	13.33	41.87	0.16	3.37	16.68	0.52	92	65	0.04	5.12	15	33	23	72	16	87	409	20	121	15	2	1	262	53	11	21	12	16.87
CLI004	1.01	2.19	13.36	43.55	0.19	3.46	15.57	0.56	92	66	0.04	5.19	21	33	18	68	17	88	418	20	134	16	2	3	291	49	26	19	14	15.98
CLI005	0.86	4.76	15.20	46.95	0.26	3.59	12.66	0.63	106	83	0.04	5.92	19	37	19	62	19	92	430	23	145	16	2	3	314	55	56	26	14	9.50
CLI006	1.12	2.60	12.43	44.72	0.37	3.68	16.31	0.54	87	65	0.04	4.79	17	32	15	65	16	92	598	22	150	15	2	1	348	48	51	18	13	13.47
CLI007	0.98	2.82	13.29	42.99	0.25	3.70	20.48	0.56	86	66	0.04	5.17	15	30	16	74	16	95	585	20	123	15	2	2	248	51	41	15	13	11.52
CLI008	1.19	2.25	15.04	46.13	0.26	4.25	13.52	0.60	102	72	0.04	5.88	18	36	15	81	18	102	495	22	139	16	1	2	282	56	26	23	14	12.77
CLI009	0.84	2.48	11.16	38.73	0.21	3.00	19.47	0.48	77	53	0.03	4.12	14	27	16	62	13	77	490	18	118	14	1	2	226	48	11	18	12	19.66
CLI010	0.94	2.64	11.85	42.88	0.20	3.62	17.27	0.54	82	64	0.04	4.69	18	30	12	65	14	85	400	21	128	15	2	2	231	43	25	21	13	16.68
CLI011	0.99	2.81	14.29	44.75	0.28	3.34	17.86	0.60	103	79	0.04	5.77	20	35	21	66	18	99	570	23	142	16	2	2	281	53	71	20	16	9.84
CLI012	0.93	2.14	15.11	50.47	0.20	4.12	10.69	0.65	104	73	0.03	5.46	21	35	15	63	19	110	358	24	163	17	1	3	324	67	40	17	14	11.23
CLI013	1.15	2.21	14.45	45.79	0.21	3.86	14.28	0.60	95	72	0.04	5.89	19	35	19	70	18	91	391	22	143	16	2	3	276	60	28	22	13	13.12
CLI014	1.19	2.12	16.01	47.50	0.22	4.50	11.05	0.60	103	76	0.04	6.21	22	38	23	77	20	104	372	21	136	16	2	3	280	54	26	24	14	11.71
CLI015	0.98	2.60	14.98	47.59	0.21	3.71	13.97	0.62	104	77	0.04	5.73	65	36	25	66	18	106	448	23	156	17	2	2	281	54	70	22	14	10.92
CLI017	0.44	2.85	13.50	44.27	0.13	3.53	14.98	0.58	96	65	0.03	4.80	20	31	13	59	17	105	547	21	143	16	2	3	270	56	30	13	13	15.81
CLI018	0.86	2.62	15.39	46.61	0.29	3.79	16.02	0.62	107	78	0.04	5.88	17	36	17	63	19	111	537	23	148	16	2	2	313	54	58	23	14	9.12
CLI019	0.90	2.45	12.84	40.66	0.25	3.62	17.85	0.52	89	62	0.03	4.88	17	31	13	78	15	86	462	19	119	15	2	2	229	40	13	19	11	17.53
CLI020	0.99	2.52	14.11	46.12	0.20	3.99	13.17	0.58	100	70	0.04	5.41	17	34	16	68	18	95	432	21	150	16	1	1	264	50	26	19	13	13.96
CLI021	0.86	2.62	12.98	41.54	0.18	3.54	16.29	0.52	93	63	0.03	4.97	16	31	20	69	16	93	409	20	127	15	2	2	259	42	21	19	13	17.75
CLI022	0.94	3.86	14.94	46.64	0.28	3.65	15.16	0.60	105	77	0.04	5.73	21	37	18	69	18	100	556	23	148	17	2	2	281	52	63	19	15	8.83
CLI023	0.55	2.82	13.75	42.92	0.15	3.62	14.84	0.56	100	68	0.04	5.27	14	32	18	61	17	101	496	20	137	16	2	3	280	62	15	18	13	16.86
CLI024	0.70	5.73	14.11	45.25	0.23	3.55	14.00	0.61	104	74	0.04	5.74	20	38	22	69	18	89	1167	24	149	16	2	4	302	62	35	13	15	11.46
CLI025	0.98	2.12	14.68	48.62	0.27	4.25	12.64	0.62	99	71	0.04	5.80	22	34	19	69	19	98	445	23	164	17	2	1	292	62	56	20	14	11.53
CLI026	0.90	2.20	14.31	44.98	0.23	4.03	14.42	0.58	98	68	0.04	5.53	11	33	23	71	18	95	446	21	142	16	2	3	278	51	15	19	14	14.56
CLI027	0.69	2.23	15.05	48.73	0.23	4.13	12.74	0.60	102	73	0.04	5.74	16	38	22	69	18	102	741	22	146	16	2	1	284	57	35	23	15	11.06
CLI028	0.76	2.45	15.38	46.47	0.33	3.63	16.46	0.61	109	83	0.04	5.75	20	36	15	66	19	116	594	24	151	17	2	2	316	57	42	20	15	8.88
CLI029	0.92	2.57	12.59	39.93	0.21	3.38	17.98	0.50	91	63	0.03	4.73	13	33	16	81	15	89	485	20	123	15	2	0	257	48	14	19	13	18.21
CLI030	0.80	4.56	15.62	46.86	0.13	4.14	10.54	0.60	109	78	0.04	6.22	16	38	23	60	19	104	990	23	145	16	2	1	292	58	28	18	15	11.30
CLI031	0.60	3.67	14.36	46.25	0.17	4.21	14.36	0.64	100	72	0.04	5.50	22	35	15	56	18	108	837	23	153	17	2	2	301	56	49	14	15	12.08
CLI032	0.80	3.00	11.86	38.61	0.18	3.25	19.08	0.50	87	57	0.04	4.69	14	31	16	63	16	86	485	20	123	15	2	0	267	48	13	19	13	19.49
CLI033	0.74	2.71	15.32	46.45	0.26	3.71	17.30	0.61	113	86	0.04	5.95	19	38	20	67	20	119	753	25	160	17	2	1	317	64	71	22	16	7.87
CLI034	0.48	2.25	14.13	44.47	0.15	3.54	14.72	0.57	103	71	0.04	5.47	15	34	12	62	18	101	542	21	143	16	1	3	274	52	13	22	13	15.57
CLI035	0.92	1.69	17.88	56.50	0.32	4.41	3.78	0.74	122	87	0.03	7.23	14	36	22	54	21	114	173	27	266	20	1	3	368	59	3	32	15	6.96
CLI036	0.74	1.94	16.86	55.24	0.15	4.33	5.29	0.70	117	87	0.03	6.57	13	37	18	70	20	116	156	23	174	19	1	2	351	58	11	21	14	8.77
CLI037	0.74	1.49	18.70	61.80	0.10	4.56	0.68	0.76	120	93	0.02	7.09	16	39	16	46	23	127	96	25	193	20	1	4	434	55	20	19	15	4.29
CLI038	0.88	2.69	14.13	47.35	0.34	3.75	15.05	0.62	101	83	0.04	5.94	16	33	21	56	16	106	484	23	165	18	2	3	330	50	21	38	15	9.25

CLI039	1.06	1.63	18.18	61.55	0.06	3.42	1.02	0.86	121	97	0.05	7.14	19	41	18	67	23	127	257	26	196	20	1	4	508	77	33	77	16	5.71
CLI040	0.81	1.80	18.72	57.37	0.12	4.36	2.12	0.74	128	92	0.02	7.22	15	43	23	58	22	120	291	24	188	20	1	5	371	60	13	28	15	6.48
CLI041	0.76	1.42	18.46	62.53	0.08	4.87	0.40	0.78	117	93	0.02	6.38	15	36	11	45	23	142	102	25	198	20	1	5	450	64	26	15	15	4.53
CLI042	0.83	2.17	17.70	58.78	0.14	4.55	1.52	0.76	115	95	0.02	6.34	14	38	11	44	22	132	126	25	189	20	2	5	403	60	14	16	15	7.33
CLI043	0.90	1.91	19.61	57.25	0.16	4.70	0.86	0.73	138	102	0.03	7.95	17	46	24	74	24	129	95	23	183	20	3	4	406	60	12	33	16	6.23
CLI044	1.00	3.55	13.48	44.28	0.21	3.38	17.96	0.57	83	76	0.04	5.17	12	31	20	58	16	91	530	20	137	17	1	4	273	48	41	20	14	10.51
CLI045	0.71	1.52	19.25	60.56	0.08	5.14	0.55	0.78	128	97	0.02	7.20	18	45	20	50	25	146	125	31	194	20	2	5	460	69	26	17	16	4.99
CLI046	0.62	1.85	17.59	59.60	0.15	4.42	2.19	0.76	139	98	0.02	7.34	13	40	27	73	21	120	185	23	184	19	2	4	403	49	11	17	14	6.13
CLI047	0.60	2.13	17.51	59.64	0.12	4.50	1.64	0.75	118	88	0.03	6.72	20	43	25	66	23	130	533	24	191	20	1	3	369	66	24	18	15	6.61
CLI048	0.42	2.22	13.92	48.55	0.17	3.62	11.86	0.57	96	71	0.03	5.44	9	31	20	56	17	101	596	20	155	17	1	3	277	52	8	21	14	13.44
CLI049	0.48	2.39	15.00	52.41	0.18	3.91	12.86	0.63	128	98	0.03	5.90	16	43	19	62	23	122	141	24	183	20	2	4	388	62	18	26	16	5.95
CLI050	0.82	2.07	16.80	54.67	0.20	4.22	5.37	0.66	115	87	0.03	6.59	14	41	22	59	21	122	410	24	180	18	1	4	371	55	8	18	15	8.49
CLI051	1.17	3.79	10.72	42.46	0.27	2.58	21.68	0.52	54	60	0.04	4.12	17	24	12	60	13	64	567	20	150	16	2	2	302	48	61	8	13	12.39
CLI052	1.04	2.26	18.26	56.41	0.11	4.70	2.56	0.82	130	95	0.03	7.54	23	54	22	60	22	125	120	28	193	21	2	4	448	71	10	21	16	7.15
CLI053	1.21	2.38	18.27	57.22	0.14	4.94	2.11	0.78	127	96	0.03	6.92	17	42	19	63	22	136	159	24	185	20	3	4	405	66	16	22	15	6.99
CLI054	1.09	1.71	17.13	61.68	0.11	4.13	2.01	0.76	121	91	0.03	6.44	20	40	14	55	21	123	127	29	215	20	2	5	443	61	22	20	15	5.20
CLI055	0.38	2.75	14.59	48.71	0.20	3.56	13.32	0.60	102	84	0.04	5.80	13	35	19	54	18	111	1251	22	150	17	1	2	320	59	17	16	16	9.93
CLI056	0.78	2.82	13.12	42.05	0.21	4.11	16.38	0.55	93	65	0.03	5.36	10	31	20	62	15	88	496	21	144	17	4	1	272	43	12	22	14	15.79
CLI057	0.82	2.42	9.35	37.22	0.27	3.47	22.26	0.46	73	49	0.03	3.83	9	20	11	60	11	82	561	18	125	15	1	0	213	36	26	13	12	19.49
CLI058	0.36	2.62	14.80	44.76	0.25	2.83	18.93	0.60	103	86	0.04	5.91	12	36	17	61	18	110	801	23	146	17	1	2	321	47	29	19	15	9.75

Table 2. Chemical concentrations by XRF. Major and minor elements expressed as oxides are in % m/m; Trace elements in µg/g; LOI (loss on ignition) in % m/m

	CLI-A1 (n = 29)		**CLI-A2** (n = 8)		**CLI-B** (n = 3)		**CLI-C1** (n = 3)		**CLI-C2** (n = 7)		**CLI-D** (n = 3)		CLI051	CLI057	CLI039	CLI043
	m	sd	m	sd	m	sd	m	sd	m	sd	m	sd				
Na_2O (m/m %)	1.05	0.15	0.53	0.10	0.87	0.09	0.89	0.09	0.94	0.25	0.77	0.03	1.34	1.02	1.11	0.96
MgO (m/m %)	2.92	0.45	3.05	0.53	5.56	0.70	2.06	0.23	2.17	0.28	1.54	0.05	4.33	3.02	1.71	2.03
Al_2O_3 (m/m %)	15.80	0.95	16.11	0.20	16.59	0.89	18.59	0.44	19.02	0.68	19.60	0.42	12.25	11.65	19.11	20.81
SiO_2 (m/m %)	50.90	2.30	52.55	2.44	51.33	1.05	60.03	0.32	62.40	1.68	64.23	1.07	48.53	46.37	64.70	60.75
P_2O_5 (m/m %)	0.27	0.05	0.20	0.04	0.23	0.07	0.24	0.09	0.14	0.02	0.09	0.01	0.31	0.34	0.06	0.17
K_2O (m/m %)	4.22	0.35	4.07	0.45	4.17	0.39	4.67	0.06	4.80	0.29	5.06	0.31	2.95	4.32	3.59	4.99
CaO (m/m %)	17.86	3.23	16.38	2.38	13.73	1.89	5.22	1.02	2.15	0.37	0.57	0.15	24.78	27.74	1.07	0.91
TiO_2 (m/m %)	0.65	0.03	0.67	0.02	0.68	0.01	0.76	0.04	0.82	0.03	0.81	0.01	0.59	0.57	0.90	0.77
V (µg/g)	110	7	117	9	118	3	128	3	134	8	127	6	62	91	127	147
Cr (µg/g)	81	7	87	10	87	5	94	1	100	4	98	2	69	61	102	108
MnO (m/m %)	0.04	0	0.04	0.01	0.04	0	0.03	0	0.03	0.01	0.02	0	0.05	0.04	0.05	0.03
Fe_2O_3 (m/m %)	6.14	0.40	6.22	0.27	6.60	0.30	7.35	0.32	7.37	0.49	7.18	0.46	4.71	4.77	7.50	8.44
Ni (µg/g)	38	2	39	3	42	1	41	3	46	6	42	5	28	25	43	49
Cu (µg/g)	21	4	19	3	24	3	23	2	22	6	16	5	14	14	19	26
Zn (µg/g)	78	9	67	4	71	6	66	9	64	10	49	3	69	75	70	79
Ga (µg/g)	20	1	21	2	21	1	23	1	23	1	25	1	15	14	24	26
Rb (µg/g)	110	8	121	4	105	9	127	6	135	7	144	11	73	103	134	137
Sr (µg/g)	556	104	736	353	957	430	267	157	235	160	112	16	648	699	270	101
Y (µg/g)	25	1	25	1	26	1	27	2	27	2	28	3	23	23	27	24
Zr (µg/g)	161	13	171	11	163	3	223	53	205	10	203	3	171	155	206	195
Nb (µg/g)	18	1	19	1	18	0	21	1	21	1	21	0	18	19	21	21
Ba (µg/g)	320	30	342	32	335	10	393	12	431	31	467	14	345	265	534	431
Ce (µg/g)	60	6	63	6	65	4	62	2	66	7	65	8	55	45	81	64
Pb (µg/g)	24	4	21	5	21	8	26	7	21	4	18	2	9	16	81	35
Th (µg/g)	16	1	16	1	16	1	16	1	16	1	16	1	15	15	17	17

Table 3: Means (m) and standard deviation (sd) of the chemical composition groups cited in the text calculated on normalised compositions. For loners, normalised compositions

XRD fabric	Mineralogical assemblage	Individuals	Sintering stage	EFT	Petrographic fabric
Calcareous groups **CLI-A1** (n = 29)					
Fabric 1 (n = 6)	Illite-muscovite, chlorite/smectite, quartz, calcite, alkali feldspar, dolomite, plagioclase, hematite	CLI002*, 3*, 9, 21, 26, 32	NV	< 700 °C	*1.1*: CLI002, 9, 32 *1.2*: CLI003 *n.d.*: CLI021, 26
Fabric 2 (n = 5)	Illite-muscovite, chlorite/smectite, quartz, calcite, alkali feldspar, plagioclase, hematite	CLI004, 12, 13, 14, 25		< 700 °C	*1.1*: CLI012, 13 *1.2*: CLI004, 14 *n.d.*: CLI025
Fabric 3 (n = 2)	Illite-muscovite, quartz, calcite, alkali feldspar, dolomite, plagioclase, hematite	CLI029, 56		< 700 °C	*1.1*: CLI0029 *1.2*: CLI0056
Fabric 4 (n = 8)	Illite-muscovite, quartz, calcite, alkali feldspar, plagioclase, hematite	CLI001*, 6, 8, 10, 15*, 19, 20, 27	Vc-/Vc	800-850 °C	*1.1*: CLI001, 8, 10, 15, 19, 20 *1.2*: CLI027 *n.d.*: CLI006
Fabric 5 (n = 8)	Illite-muscovite, quartz, calcite, alkali feldspar, plagioclase, gehlenite, hematite, pyroxene	CLI007, 11*, 18, 22, 28, 33*, 38, 44	Vc	850-950 °C	*1.1*: CLI007, 11, 18, 28, 33, 38, 44 *n.d.*: CLI022
CLI-A2 (n = 8)					
Fabric 1 (n = 3)	Illite-muscovite, chlorite/smectite, quartz, calcite, alkali feldspar, dolomite, plagioclase, hematite	CLI017, 23*, 49	NV	< 700 °C	*1.1*: CLI023 *1.2*: CLI017 *2*: CLI049
Fabric 2 (n = 2)	Illite-muscovite, chlorite/smectite, quartz, calcite, alkali feldspar, plagioclase, hematite	CLI034*, 48	NV	< 700 °C	*1.1*: CLI034 *2*: CLI048
Fabric 3 (n = 2)	Illite-muscovite, quartz, calcite, alkali feldspar, plagioclase, hematite	CLI031*, 55	IV/Vc-	750-850 °C	*1.1*: CLI031 *1.3*: CLI055
Fabric 4 (n = 1)	Illite-muscovite, quartz, calcite, alkali feldspar, plagioclase, gehlenite, hematite, pyroxene	CLI058*	Vc	850-950 °C	*1.1*: CLI058
CLI-B (n = 3)					
Fabric 1 (n = 1)	Illite-muscovite, quartz, calcite, alkali feldspar, plagioclase, hematite	CLI030		700-800/850 °C	*1.1*: CLI030
Fabric 2 (n = 2)	Illite-muscovite, quartz, calcite, alkali feldspar, plagioclase, gehlenite, hematite, pyroxene	CLI005*, 24*	Vc	850-950 °C	*1.1*: CLI005, 24

Loners (n = 2)					
Fabric 1 (n = 1)	Illite-muscovite (?), quartz, calcite, alkali feldspar, gehlenite, hematite, pyroxene, analcime	CLI051		950/1000-1050 °C	*Loner*
Fabric 1 (n = 1)	Illite-muscovite, quartz, calcite, alkali feldspar, plagioclase, hematite	CLI057		700-800/850 °C	*1.1*
Low calcareous groups **CLI-C1** (n = 3)					
Fabric 1 (n = 3)	Illite-muscovite, chlorite/smectite, quartz, calcite, alkali feldspar, plagioclase, hematite	CLI035, 36, 50		< 700 °C	*1.1*: CLI035 *2*: CLI036, 50
CLI-C2 (n = 7)					
Fabric 1 (n = 1)	Illite-muscovite, chlorite/smectite, quartz, calcite, alkali feldspar, plagioclase, hematite, hydrotalcite	CLI042		< 700 °C (?)	*2*: CLI042
Fabric 2 (n = 4)	Illite-muscovite, chlorite/smectite, quartz, calcite, alkali feldspar, plagioclase, hematite	CLI040, 46*, 47, 52	NV	< 700 °C	*2*: CLI040, 46, 52 *n.d.*: CLI047
Fabric 3 (n = 2)	Illite-muscovite, quartz, calcite, alkali feldspar, plagioclase, hematite	CLI053*, 54	NV	700-750 °C	*2*: CLI053, 54
CLI-D (n = 3)					
Fabric 1 (n = 2)	Illite-muscovite, chlorite/smectite, quartz, calcite (?), alkali feldspar, plagioclase, hematite	CLI037, 41		< 700 °C	*2*: CLI041 *n.d.*: CLI037
Fabric 2 (n = 1)	Illite-muscovite, quartz, calcite, alkali feldspar, plagioclase, hematite	CLI045*	NV	700-750 °C	*2*: CLI045
Loners (n = 2)					
Fabric 1 (n = 1)	Illite-muscovite, chlorite/smectite, quartz, calcite, alkali feldspar, plagioclase, hematite	CLI039		< 700 °C	*Loner*
Fabric 1 (n = 1)	Illite-muscovite, chlorite/smectite, quartz, calcite, alkali feldspar, plagioclase, hematite	CLI043		< 700 °C	*2*
Not analysed by XRF and XRD (n = 6)					
Fabric 1 (n = 6)	-	CLI059, 60, 61, 62, 63, 64	-	-	*1.1*: CLI059, 60, 61, 62 *1.2*: CLI063, 64

Table 4. Mineralogical fabrics, sintering state and estimated EFT of the analysed samples from Castellar de Librilla based on XRD and SEM results. EFT: equivalent firing temperature. * Individual observed by SEM (n = 15). In red: individuals with high Sr values. NV: no vitrification; IV: initial vitrification; Vc-: continuous vitrification (less developed); Vc: continuous vitrification.

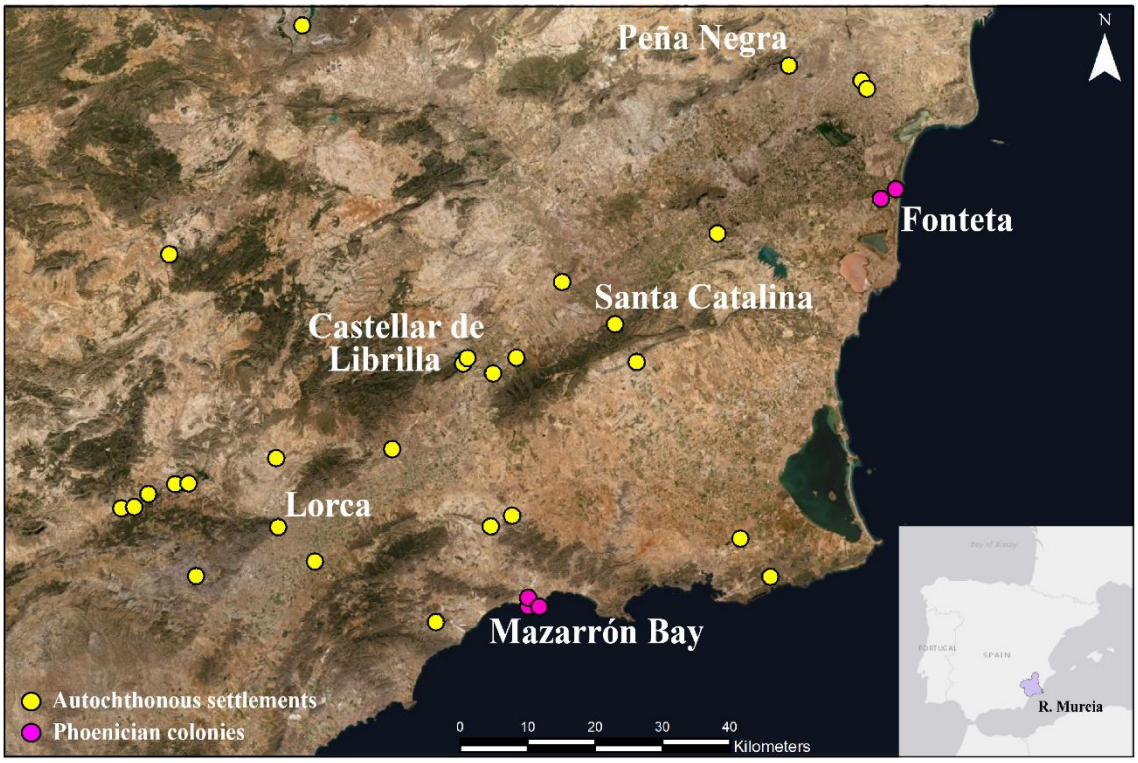

Fig. 1 Location of Castellar de Librilla in the context of Iberian Southeast, the main autochthonous settlements and Phoenician colonies cited in the text (Source: Cutillas-Victoria after MDT Spanish National Geographic Institute).

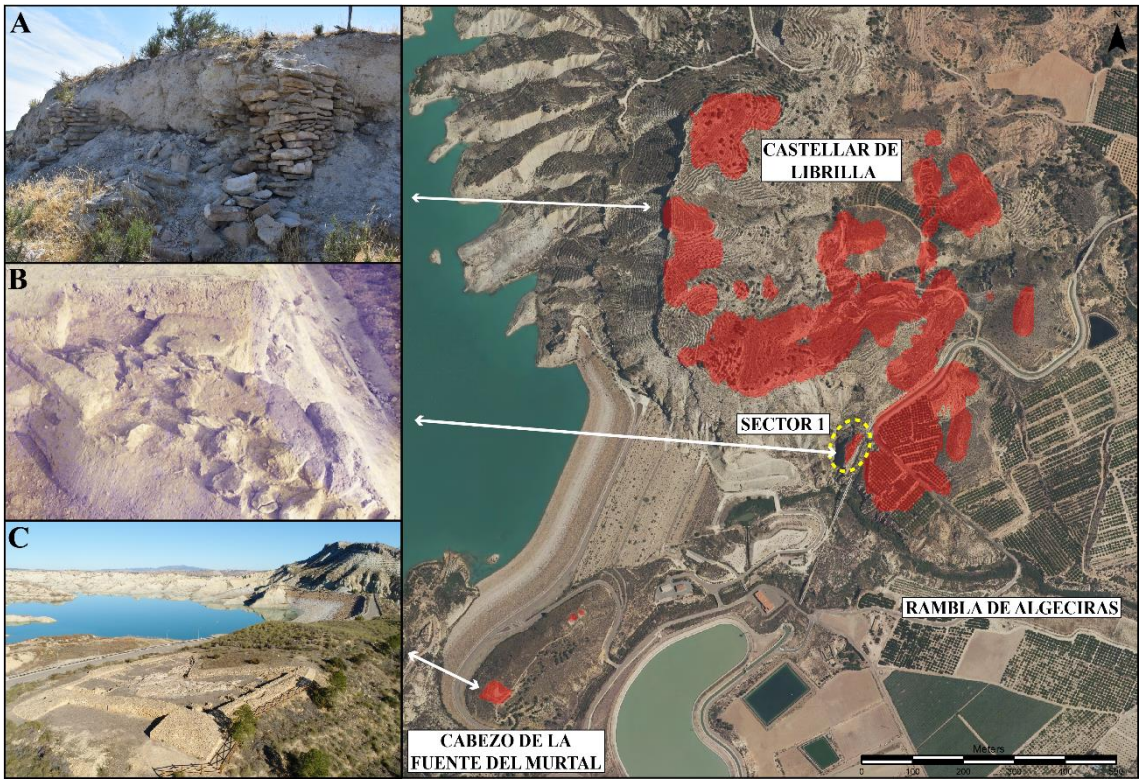

Fig. 2 Distribution of settled areas of Castellar de Librilla (Source: Cutillas-Victoria after MDT Spanish National Geographic Institute). A) Section with Early Iron Age structures from Sector 13 (Source: authors); B) Part of the pottery kiln excavated in the 1980s (courtesy of M.M. Ros); C) Aerial view of Cabezo de la

Fuente del Murtal fortress with Castella de Librilla at the top right corner (Source: Alhama de Murcia Town Hall).

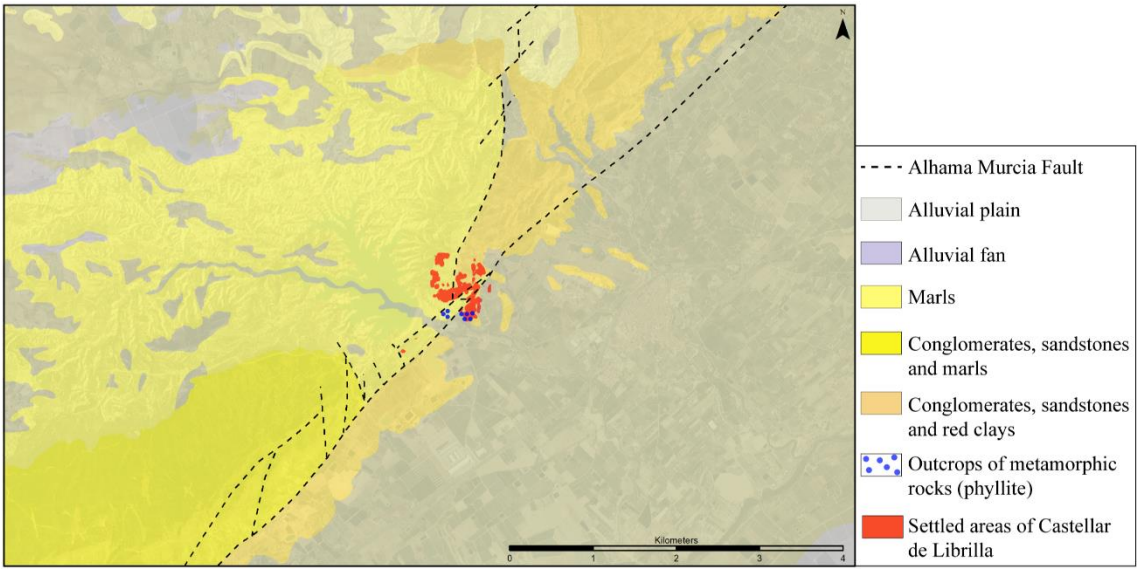

Fig. 3 Geological map of Rambla de Algeciras area, with the Castellar de Librilla settlement (Source: Cutillas-Victoria based on Geological and Mining Institute of Spain, Sheet number 933 (Kampschuur et al. 1972)).

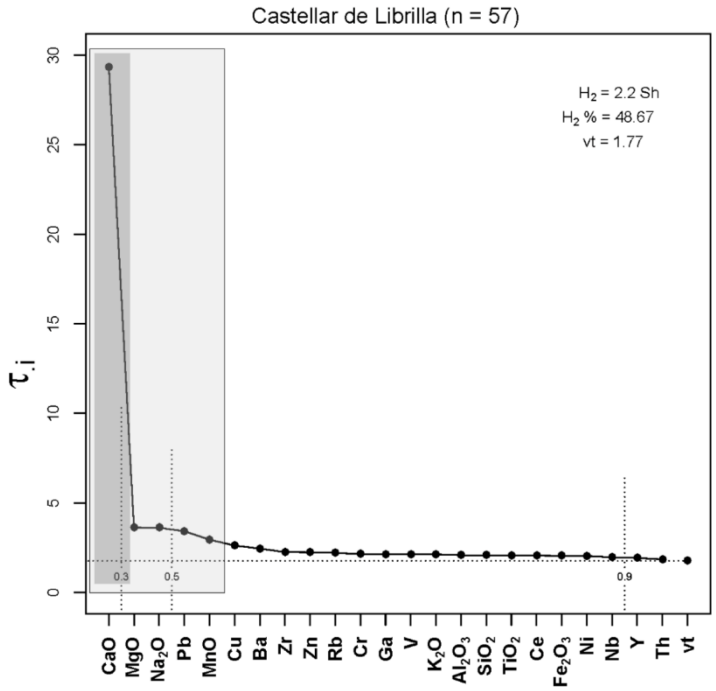

Fig. 4 Compositional evenness plot for the 57 samples analysed. H_2: information entropy (in shanons, Sh); H_2 %: percentage on the possible maximum; vt: total variation; $\tau_{i.}$ trace of the covariance matrix in alr transformation using that element as the divisor.

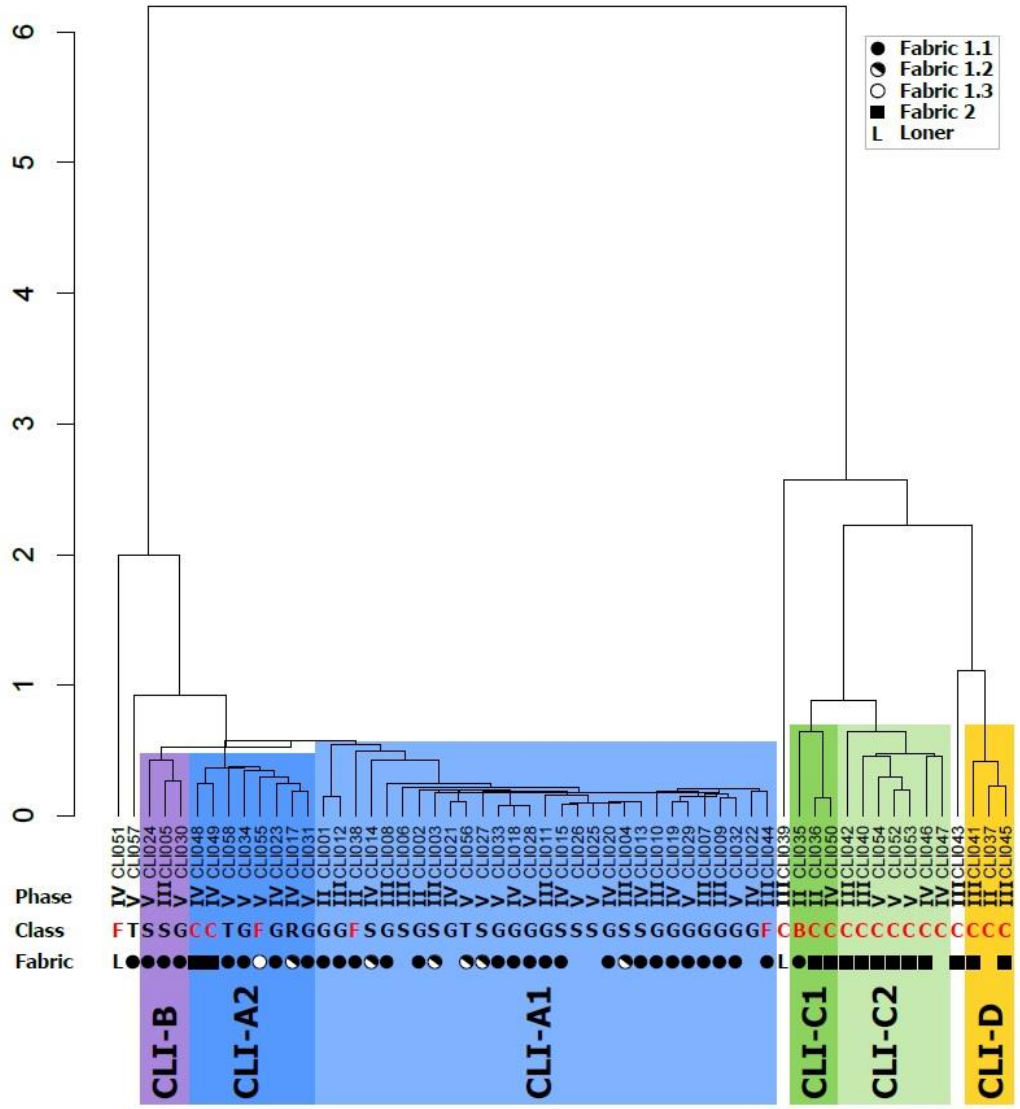

Fig. 5 Dendrogram of 57 individuals after a cluster analysis performed on the subcomposition Na_2O, MgO, Al_2O_3, SiO_2, K_2O, CaO, TiO_2, V, Cr, MnO, Fe_2O_3, Ni, Cu, Zn, Ga, Rb, Y, Zr, Nb, Ba, Ce, Pb, and Th, clr transformed, including chronological phase, ceramic class, and petrographic fabric. G: Grey pottery; R: Red slip ware; R: Red common ware; T: Transport ware; B: Burnished LBA; C: Cooking ware; F: Furniture ware. Black class indication: wheel-made; Red class indication: handmade

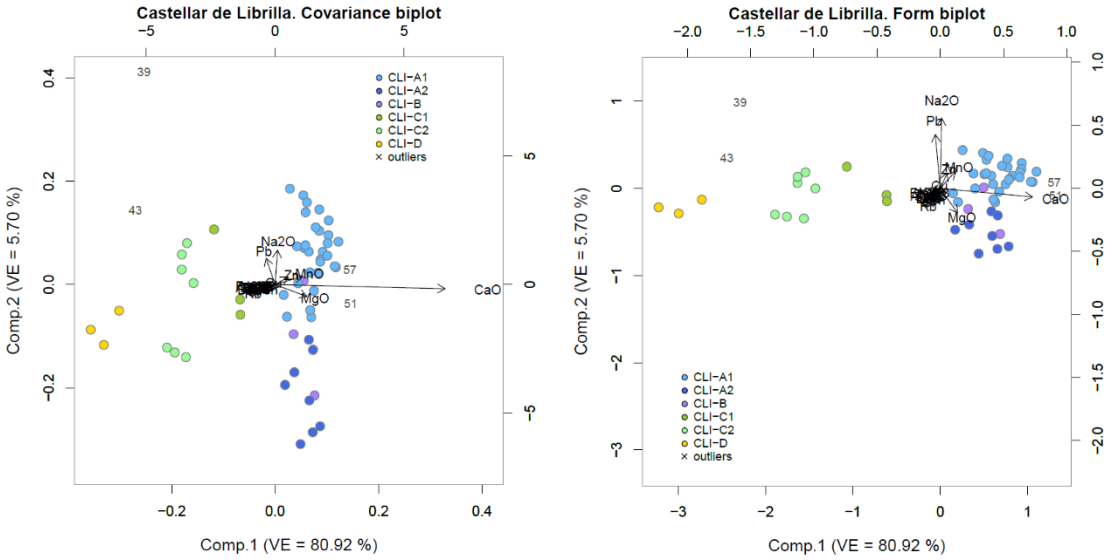

Fig. 6 Biplots of the singular value decomposition on the double centred clr transformed subcomposition Na_2O, MgO, Al_2O_3, SiO_2, K_2O, CaO, TiO_2, V, Cr, MnO, Fe_2O_3, Ni, Cu, Zn, Ga, Rb, Y, Zr, Nb, Ba, Ce, Pb, and Th. Left: covariance biplot. Right: form biplot. VE: variance explained

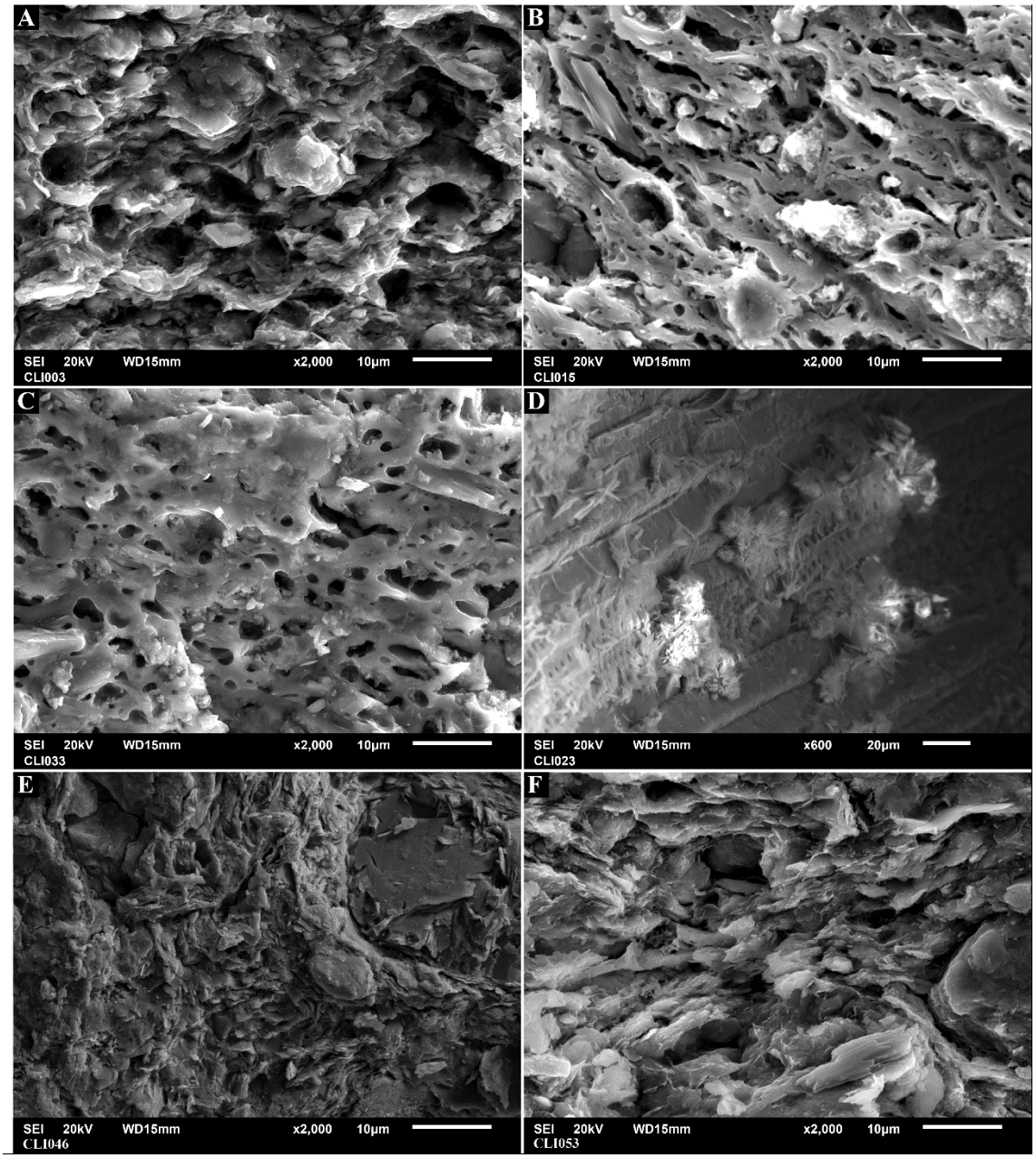

Fig. 7 SEM photomicrographs showing the different sintering stages. A) NV stage in individual CLI003 (CLI-A1, XRD fabric 1); B) Vc stage in individual CLI015 (CLI-A1, XRD fabric 4); C) Vc stage in individual CLI033 (CLI-A1, XRD fabric 5); D) Crystals of authigenic celestine in void in individual CLI023 (CLI-A2, XRD fabric 1); E) NV stage in individual CLI046 (CLI-C2, XRD fabric 2); F) NV stage in individual CLI053 (CLI-C2, XRD fabric 3).

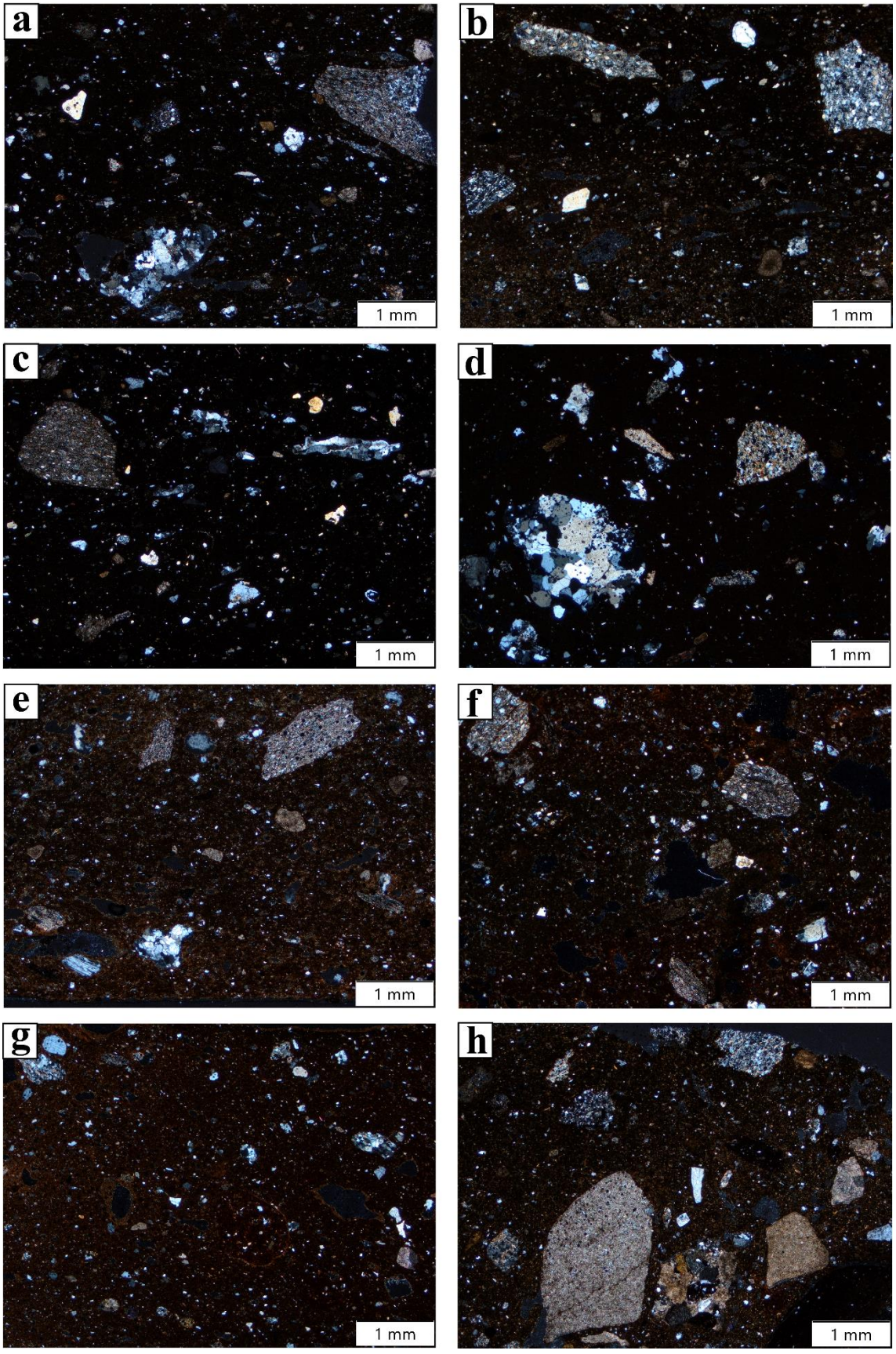

Fig. 8 Photomicrographs of Fabric group 1 identified in Castellar de Librilla ceramic thin sections, crossed polars (XP). **a** CLI005 (Fab. 1.1). **b** CLI010 (Fab. 1.1). **c** CLI030 (Fab. 1.1). **d** CLI061 (Fab. 1.1). **e** CLI004 (Fab. 1.2). **f** CLI017 (Fab. 1.2). **g** CLI056 (Fab. 1.2). **h** CLI055 (Fab. 1.3).

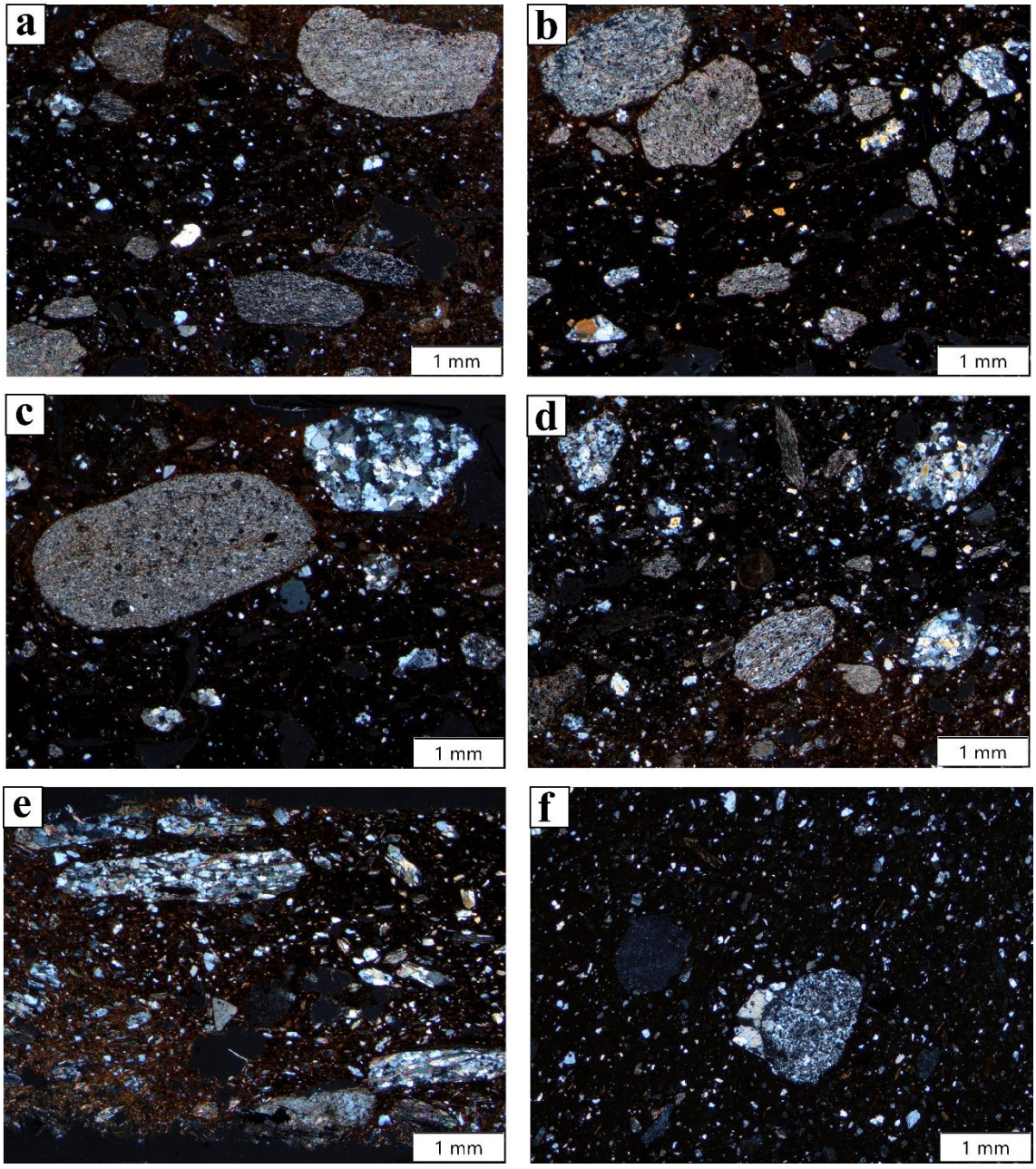

Fig. 9 Photomicrographs of Fabric Group 2 and loner individuals identified in Castellar de Librilla ceramic thin sections, crossed polars (XP). **a** CLI036 (Fab. 2). **b** CLI045 (Fab. 2). **c** CLI049 (Fab. 2). **d** CLI054 (Fab. 2). **e** CLI039 (Loner). **f** CLI051 (Loner).

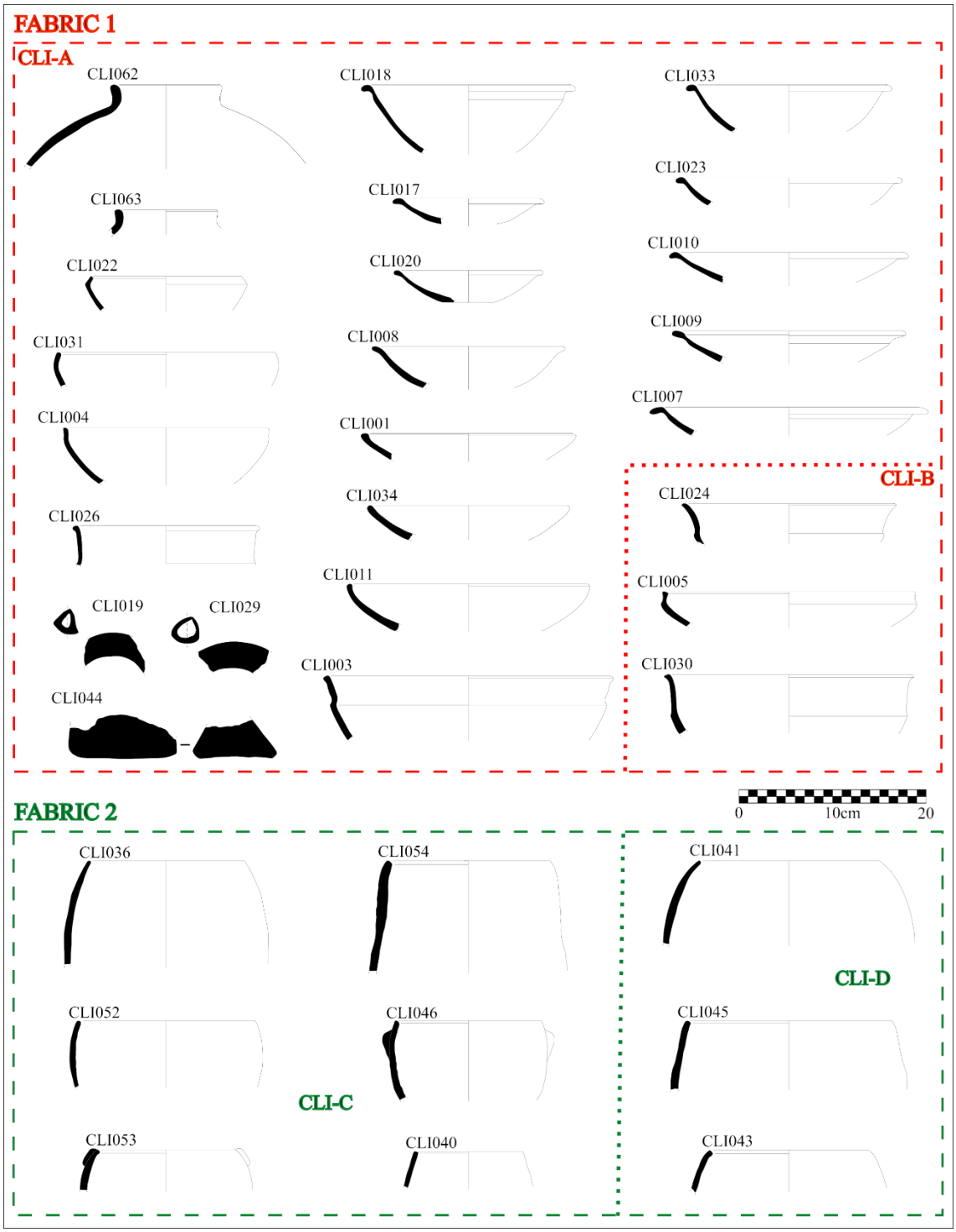

Fig. 10. Representative ceramic forms identified in Castellar de Librilla and their assignment according to their belonging to chemical groups and fabrics.

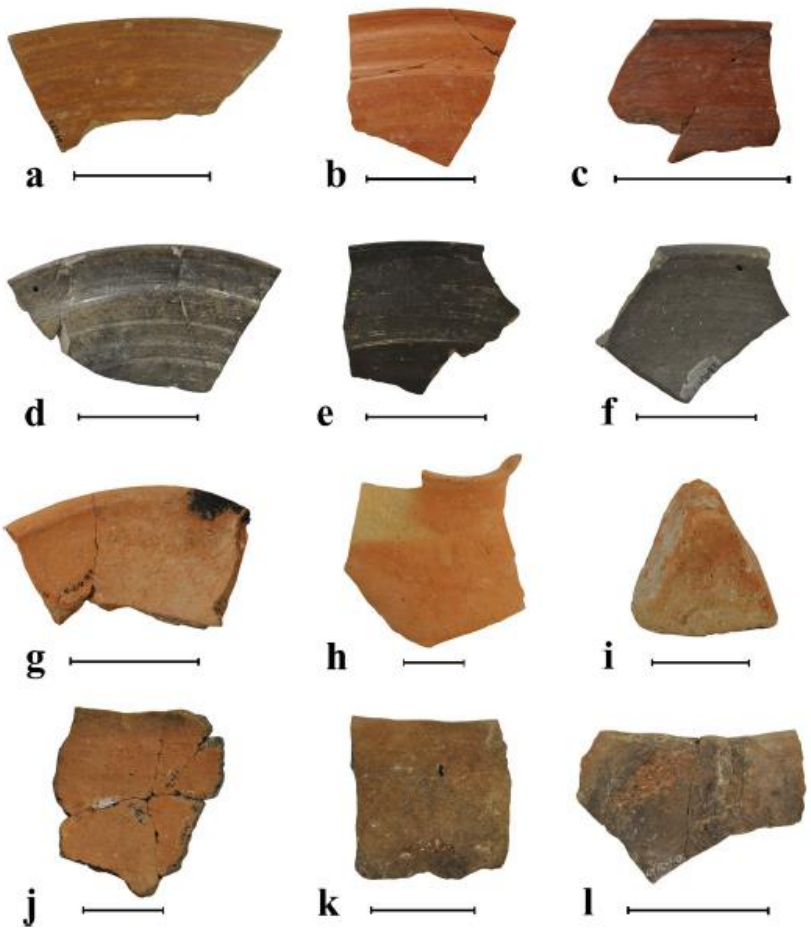

Fig. 11 Example of wares manufactured at Castellar de Librilla. **a** Red slipped plate CLI003 (CLI-A1, Pet. Fab. 1.2). **b** Red slipped plate CLI014 (CLI-A1, Pet. Fab. 1.2). **c** Red slipped plate CLI015 (CLI-A1, Pet. Fab. 1.1). **d** Grey pottery plate CLI009 (CLI-A1, Pet. Fab. 1.1). **e** Grey pottery plate CLI030 (CLI-B, Pet. Fab. 1.1). **f** Grey pottery plate CLI033 (CLI-A1, Pet. Fab. 1.1). **g** Red slipped oil lamp CLI017 (CLI-A2, Pet. Fab. 1.2). **h** Amphora CLI062 (Pet. Fab. 1.1). **i** Triangular support CLI044 (CLI-A1, Pet. Fab. 1.1). **j** Handmade cooking pot CLI036 (CLI-C1, Pet. Fab. 2). **k** Handmade cooking pot CLI053 (CLI-C2, Pet. Fab. 2). **l** Handmade cooking pot CLI045 (CLI-D, Pet. Fab. 2). Bar = 5 cm. (Photos: B. Cutillas-Victoria)